

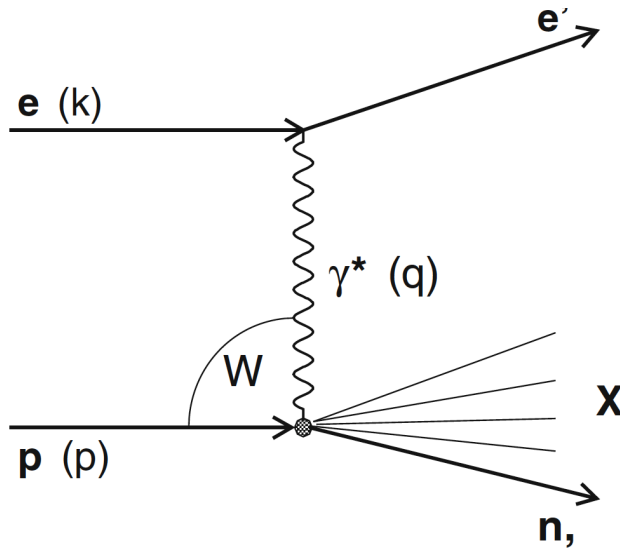
Exclusive processes with a leading neutron in e-p collisions

Fernando S. Navarra

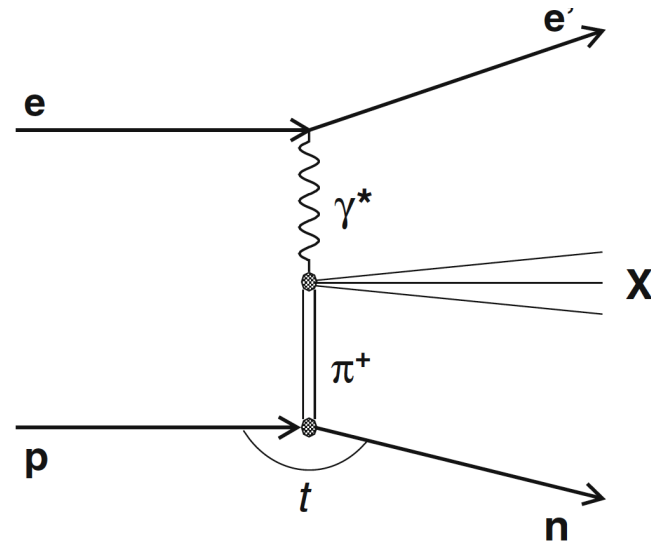
University of São Paulo

Low x Meeting 2016 6-11 June 2016
Károly Róbert College, Gyöngyös, Hungary

Leading neutrons in Deep Inelastic Scattering



normal DIS
with quark fragmentation



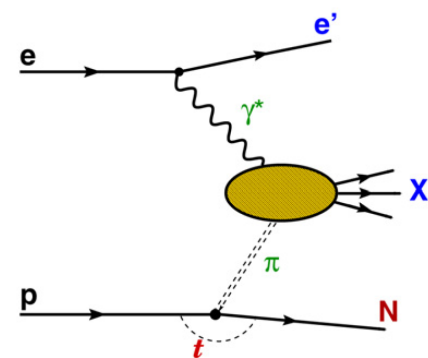
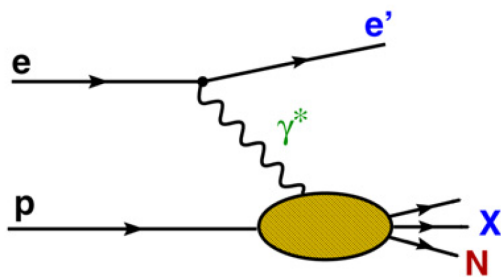
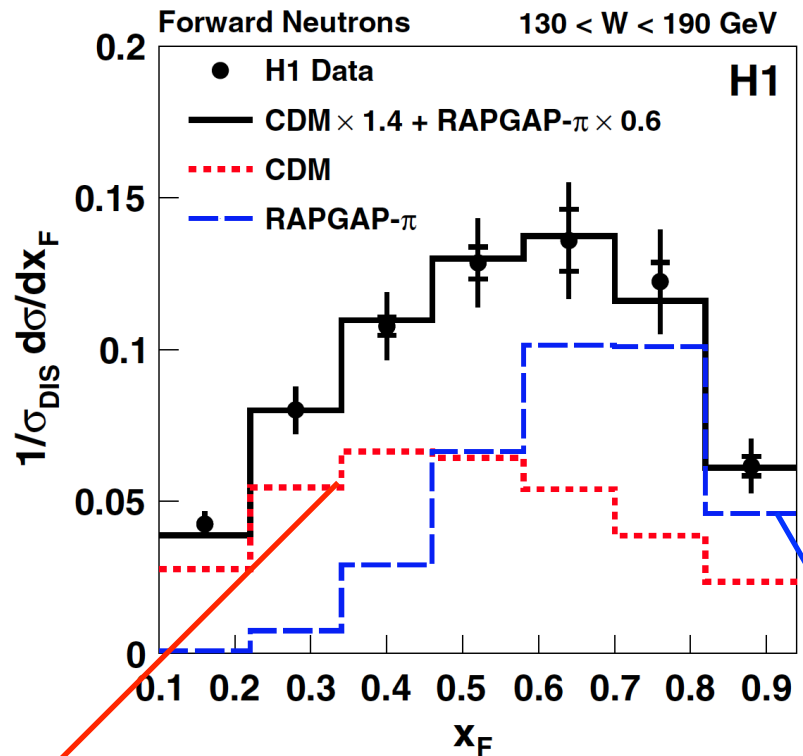
pion emission

Forward neutrons

$$\eta > 7.9$$

$$0.1 < x_F < 0.94$$

$$0 < p_T^* < 0.6 \text{ GeV}$$



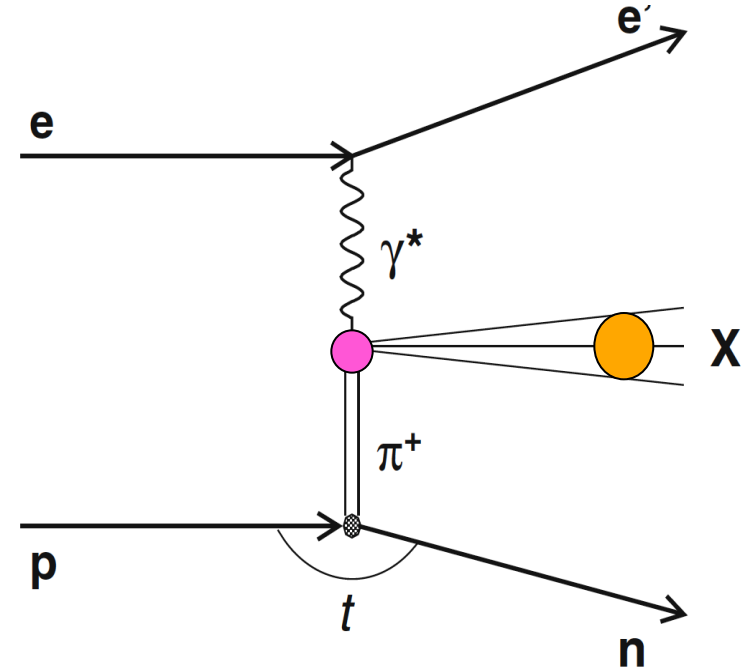
Our goal

- Pion-photon in the color dipole approach
(gluon saturation effects)

- Inclusive and exclusive processes

- Understand new HERA data:

$$e^- + p \rightarrow e^- + X + n$$



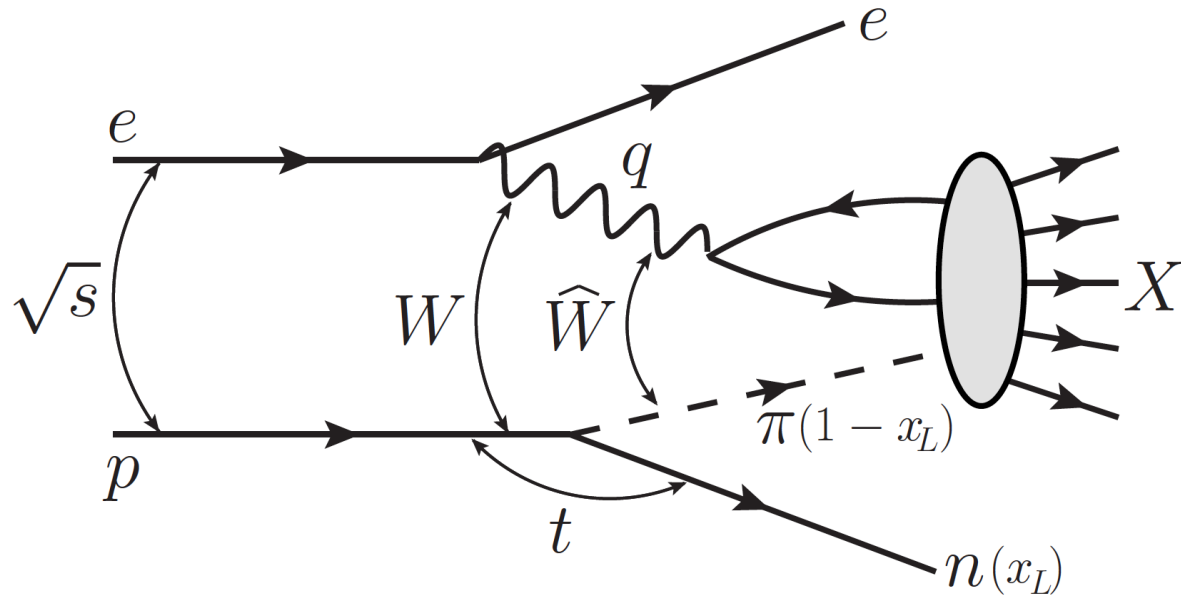
V. Andreev et al., EJPC 74, 2915 (2014)

$$e^- + p \rightarrow e^- + \rho^0 + \pi^+ + n$$

V. Andreev et al., EJPC 76, 41 (2016)

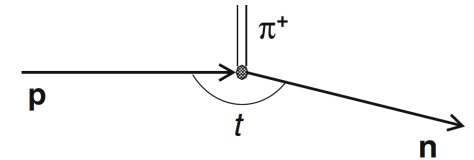
$$e^- + p \rightarrow e^- + X + n$$

$$\frac{d^2\sigma(W, Q^2, x_L, t)}{dx_L dt} = f_{\pi/p}(x_L, t) \sigma_{\gamma^* \pi}(\hat{W}^2, Q^2)$$



$$\hat{W}^2 = (1 - x_L) W^2$$

Pion splitting function



$$f_{\pi/p}(x_L, t) = \frac{1}{4\pi} \frac{2g_{p\pi p}^2}{4\pi} \frac{-t}{(t - m_\pi^2)^2} (1 - x_L)^{1-2\alpha(t)} [F(x_L, t)]^2$$

Form factors:

$$F_1(x_L, t) = \exp[R^2 \frac{(t - m_\pi^2)}{(1 - x_L)}] \quad \alpha(t) = 0 \quad \text{light cone}$$

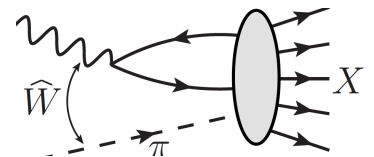
$$F_2(x_L, t) = 1 \quad \alpha(t) = \alpha_\pi(t) = t \quad \text{reggeized pion}$$

$$F_3(x_L, t) = \exp[b(t - m_\pi^2)] \quad \alpha(t) = \alpha_\pi(t) = t \quad \text{monopole}$$

$$F_4(x_L, t) = \frac{(\Lambda^2 - m_\pi^2)}{(\Lambda^2 - t^2)} \quad \alpha(t) = 0 \quad \text{dipole}$$

$$F_5(x_L, t) = [\frac{(\Lambda^2 - m_\pi^2)}{(\Lambda^2 - t^2)}]^2 \quad \alpha(t) = 0$$

Pion-photon cross section:



$$\sigma_{\gamma^* \pi}(\hat{x}, Q^2) = \int_0^1 dz \int d^2 r \sum_{L,T} |\Psi_{L,T}(z, r, Q^2)|^2 \sigma_{d\pi}(\hat{x}, r)$$

Photon wave function:

$$|\psi_L(z, r)|^2 = \frac{3\alpha_{em}}{\pi^2} \sum_f e_f^2 4Q^2 z^2 (1-z)^2 K_0^2(\epsilon r) \quad \epsilon^2 = z(1-z)Q^2 + m_f^2$$

$$|\psi_T(z, r)|^2 = \frac{3\alpha_{em}}{2\pi^2} \sum_f e_f^2 \{ [z^2 + (1-z^2)\epsilon^2] K_1^2(\epsilon r) + m_f^2 K_0^2(\epsilon r) \}$$

Dipole cross section:

$$\sigma_{d\pi}(\hat{x}, r) = 2 \int d^2 b \mathcal{N}_\pi(\hat{x}, r, b) = \sigma_0 \mathcal{N}_\pi(\hat{x}, r)$$

$$\mathcal{N}_\pi(\hat{x}, r, b) = R_q \mathcal{N}_p(\hat{x}, r, b)$$

$$R_q = \frac{2}{3}$$

$$\sigma_{d\pi} = \frac{2}{3} \sigma_{dp}$$

additive quark model

Non-linear (saturation) models:

$$\mathcal{N}(r, \hat{x}) = [1 - \exp(-\frac{(Q_s(\hat{x})r)^2}{4})]$$

GBW

$$N(r, \hat{x}) = \begin{cases} \mathcal{N}_0 \left(\frac{r, Q_s}{2} \right)^{2(\gamma_s + \frac{\ln(2/rQ_s)}{\kappa \lambda Y})}, & \text{for } rQ_s(\hat{x}) \leq 2 \\ 1 - \exp^{-a \ln^2(b r Q_s)}, & \text{for } rQ_s(\hat{x}) > 2 \end{cases}$$

IIM-S

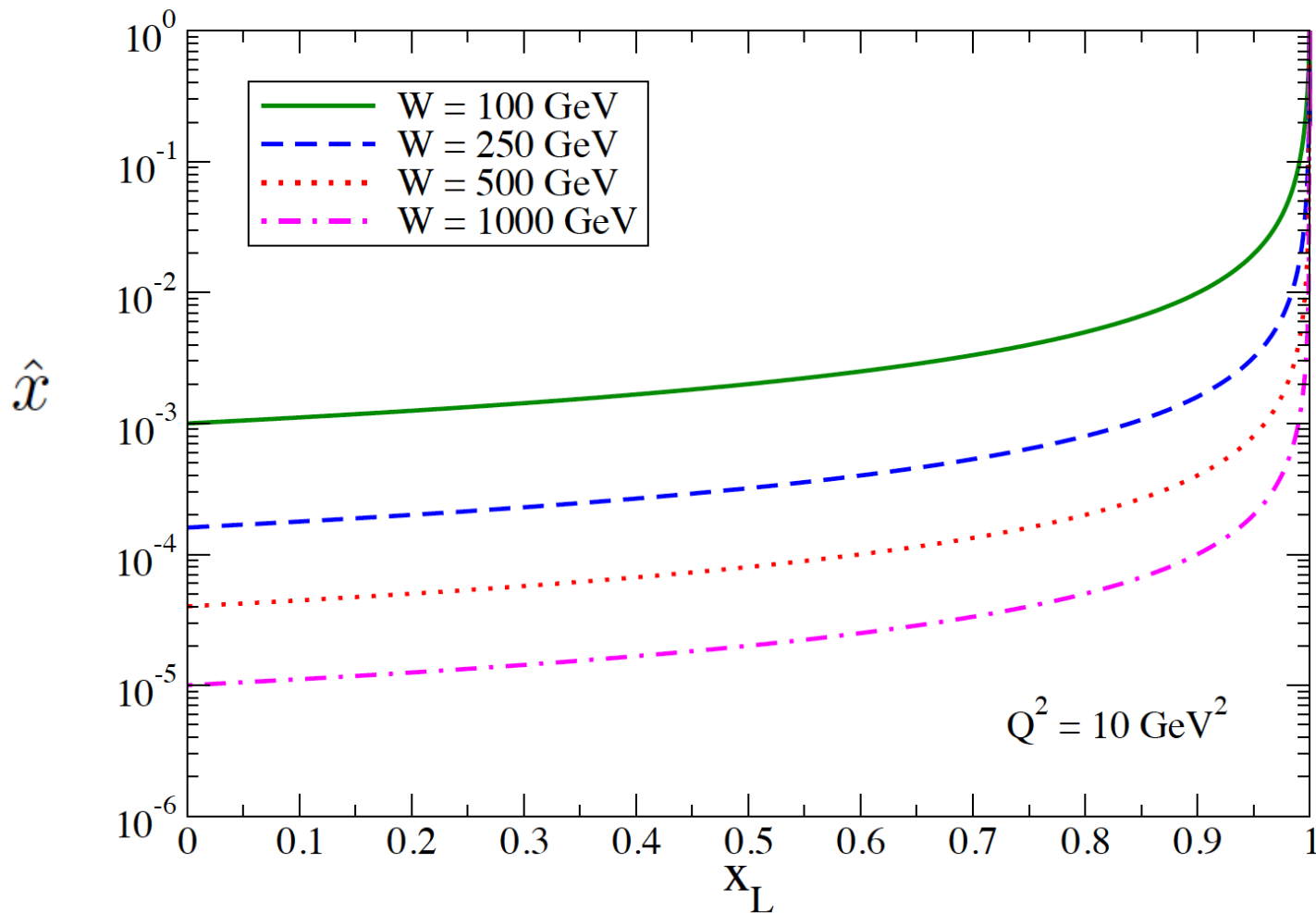
$$Q_s^2(\hat{x}) = Q_0^2 \left(\frac{x_0}{\hat{x}} \right)^\lambda$$

Linear (no saturation) model:

$$\sigma_{dip}(r, \hat{x}) = \frac{\pi^2}{3} r^2 \alpha_s \hat{x} g(x, 10/r^2)$$

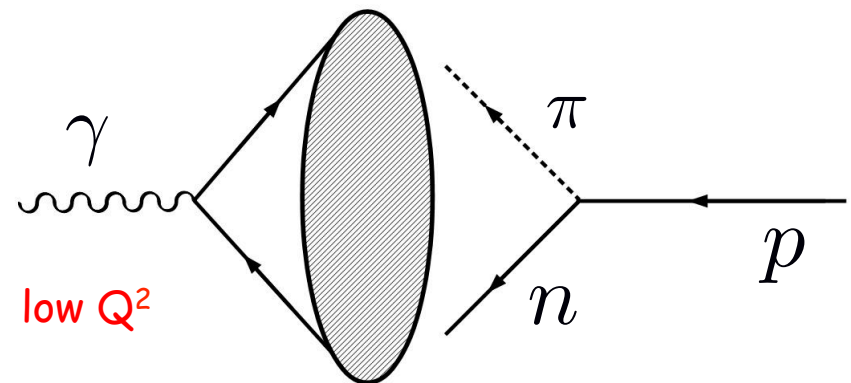
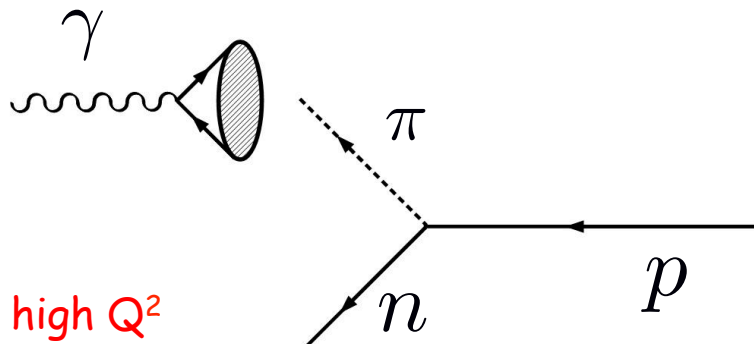
Blättel, Baym, Frankfurt, Heiselberg, Strikman, PRD (1993)

Leading neutron production can be low x physics !



$$\hat{x} = \frac{Q^2 + m_f^2}{\hat{W}^2 + Q^2} = \frac{Q^2 + m_f^2}{(1 - x_L)W^2 + Q^2}$$

Absorption effects



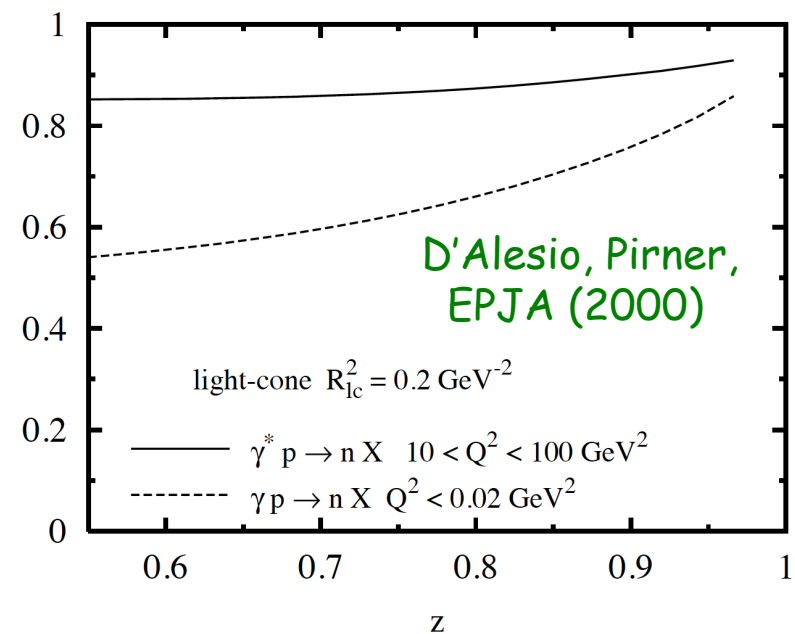
$$\frac{d^2\sigma(W, Q^2, x_L, t)}{dx_L dt} = K f_{\pi/p}(x_L, t) \sigma_{\gamma^* \pi}(\hat{W}^2, Q^2)$$

Kopeliovich, Potashnikova,
Povh, Schmidt,
PRD (2012)

$$K < 0.5$$

H1: V. Andreev et al.,
EJPC 76, 41 (2016)

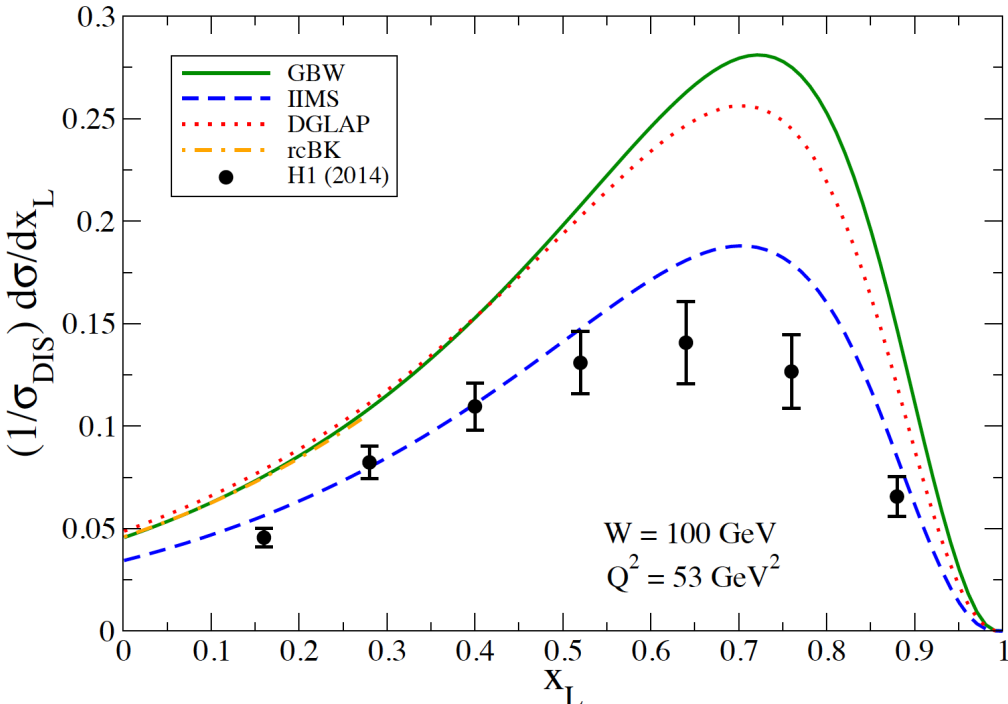
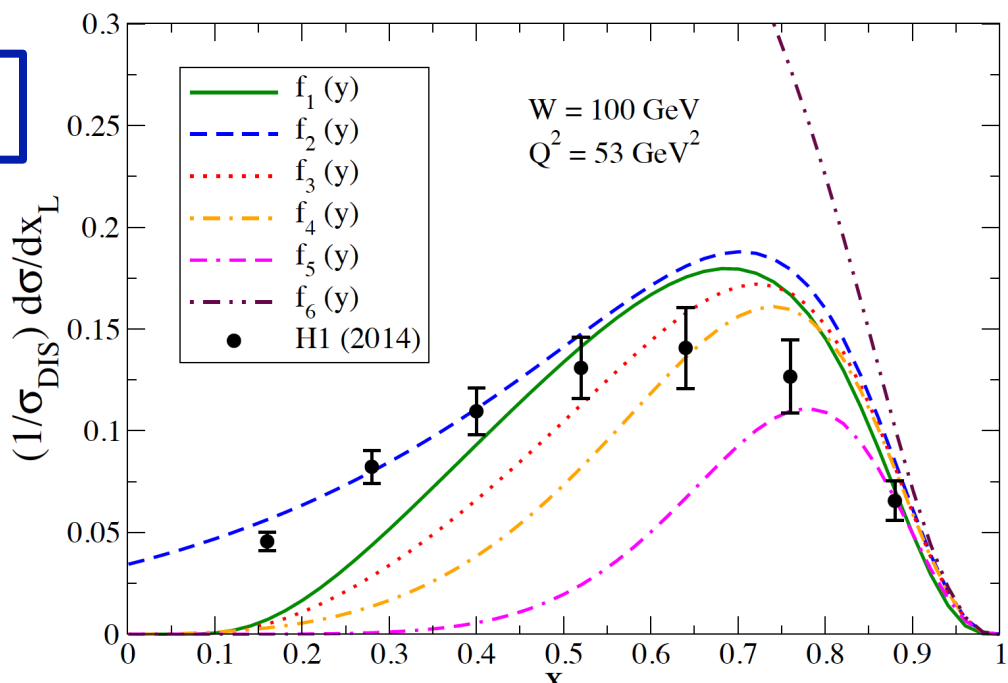
$$K = 0.44 (11)$$





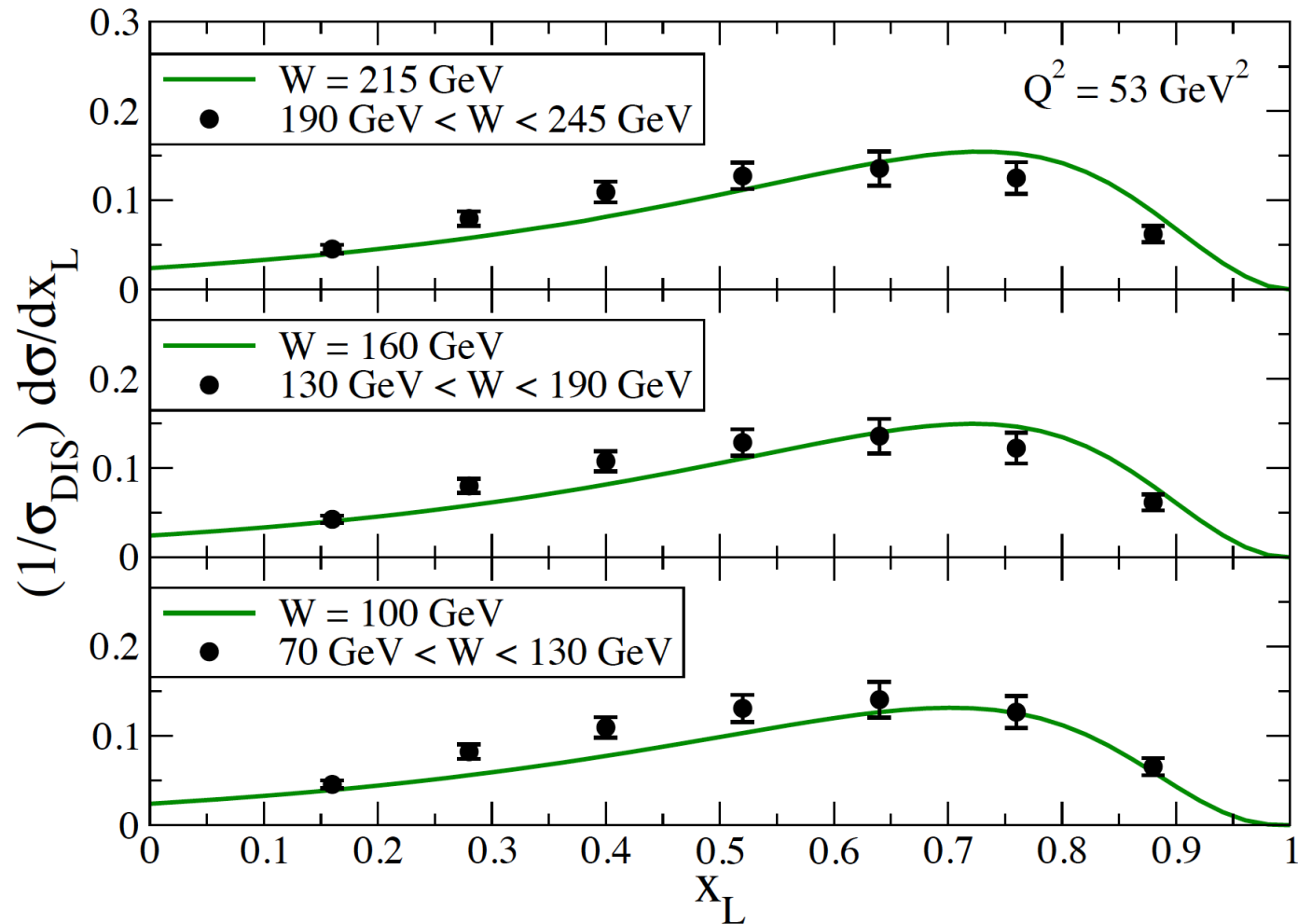
$$R_q = \frac{2}{3}$$

$$K = 1$$



$$R_q = \frac{2}{3}$$

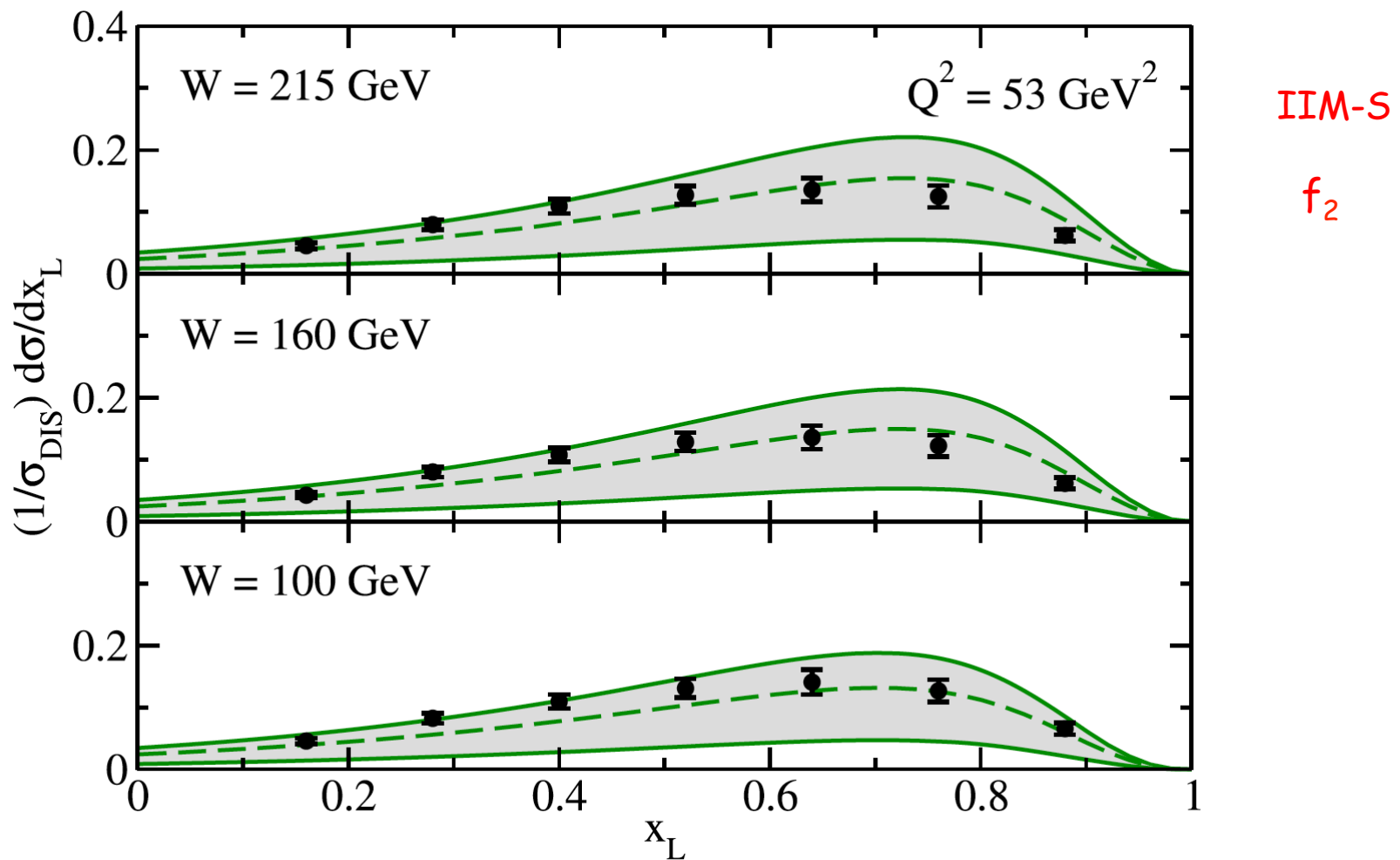
$$K = 0.7$$



*

$$\frac{1}{3} < R_q < \frac{2}{3}$$

$$0.5 < K < 1$$

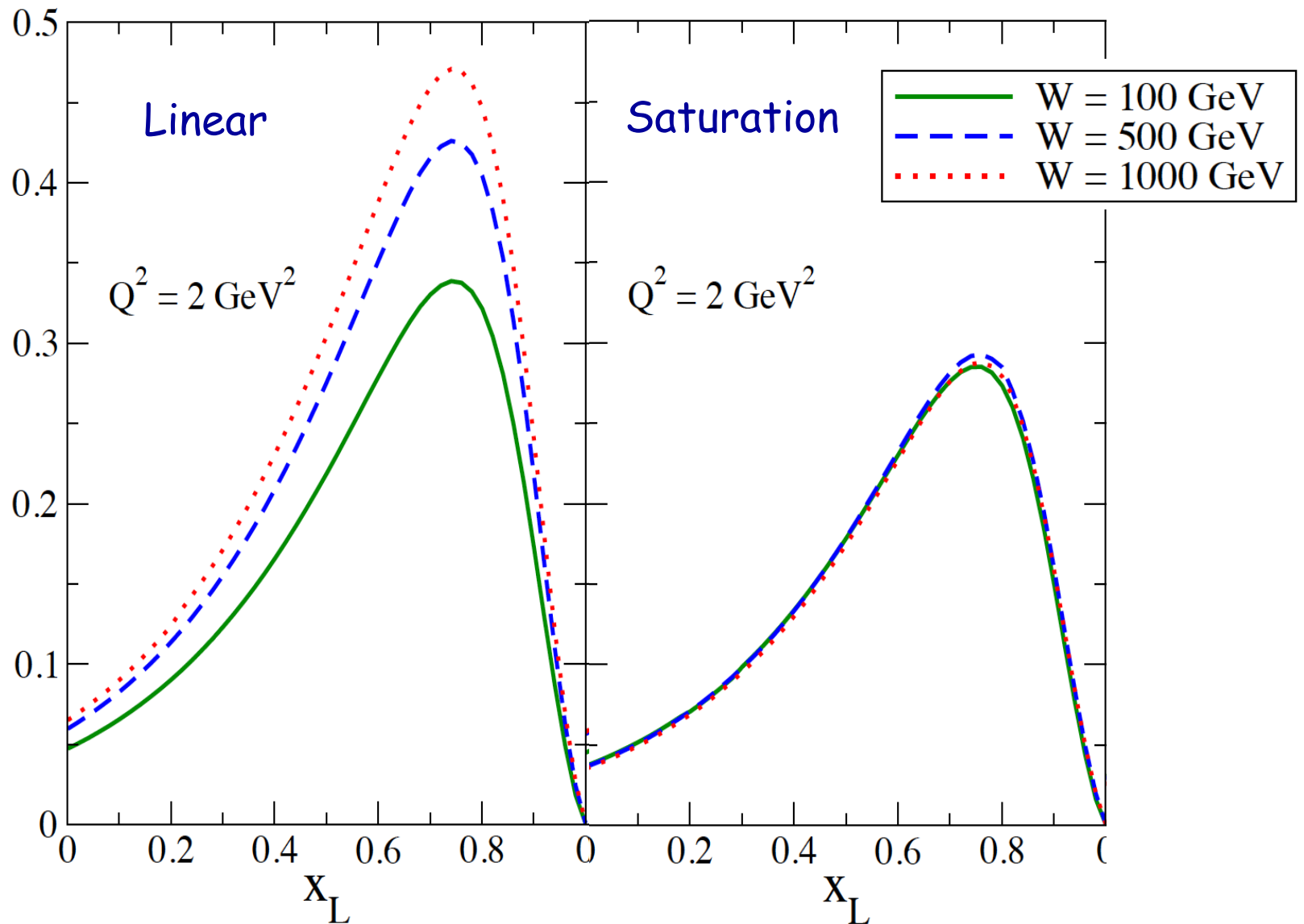


Carvalho, Gonçalves, Spiering, FSN, PLB 725 (2016) 76

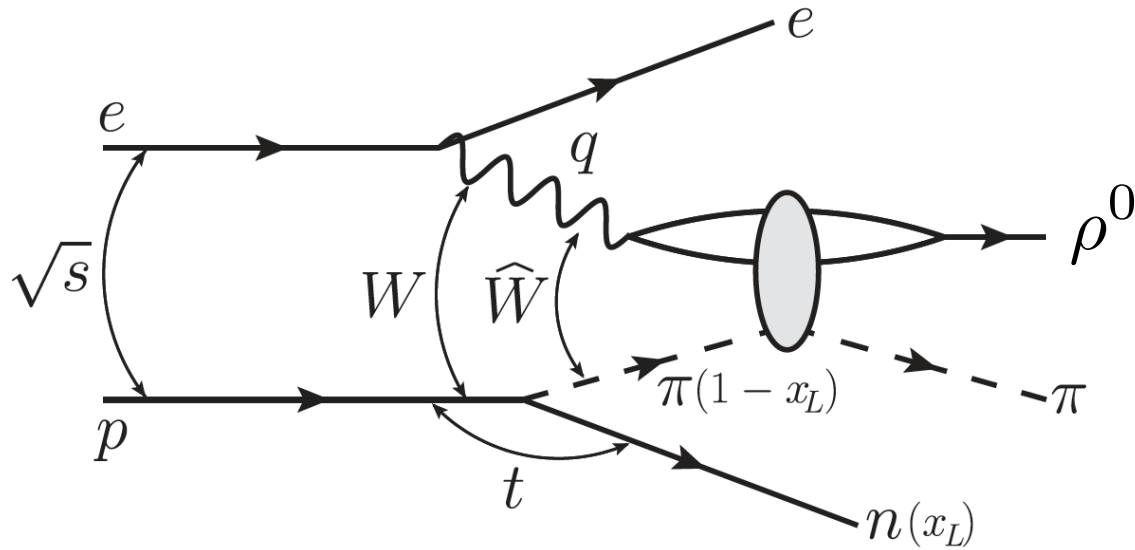
*

S. Chekanov *et al.* [ZEUS Collaboration], Nucl. Phys. **B637** 3 (2002) 3

Prediction: Feynman scaling



$$e^- + p \rightarrow e^- + \rho^0 + \pi^+ + n$$



$$\frac{d^2\sigma(W,Q^2,x_L,t)}{dx_L dt} = K f_{\pi/p}(x_L,t) \sigma_{\gamma^*\pi}(\hat{W}^2,Q^2)$$

$$\sigma(\gamma^*\pi \rightarrow E\pi) = \sum_{i=L,T} \int_{-\infty}^0 \frac{d\sigma_i}{d\hat{t}} d\hat{t} = \frac{1}{16\pi} \sum_{i=L,T} \int_{-\infty}^0 |\mathcal{A}_i^{\gamma^*\pi \rightarrow E\pi}(x,\Delta)|^2 d\hat{t}$$

$$\mathcal{A}_{T,L}^{\gamma^*\pi \rightarrow E\pi}(\hat{x}, \Delta) = i \int dz d^2\mathbf{r} d^2\mathbf{b} e^{-i[\mathbf{b}-(1-z)\mathbf{r}].\Delta} \quad (\Psi^{E*}\Psi)_{T,L} 2\mathcal{N}_\pi(\hat{x}, \mathbf{r}, \mathbf{b})$$

$$(\Psi_V^* \Psi)_T = \frac{\hat{e}_f e}{4\pi} \frac{N_c}{\pi z(1-z)} \{ m_f^2 K_0(\epsilon r) \phi_T(r, z) - [z^2 + (1-z)^2] \epsilon K_1(\epsilon r) \partial_r \phi_T(r, z) \}$$

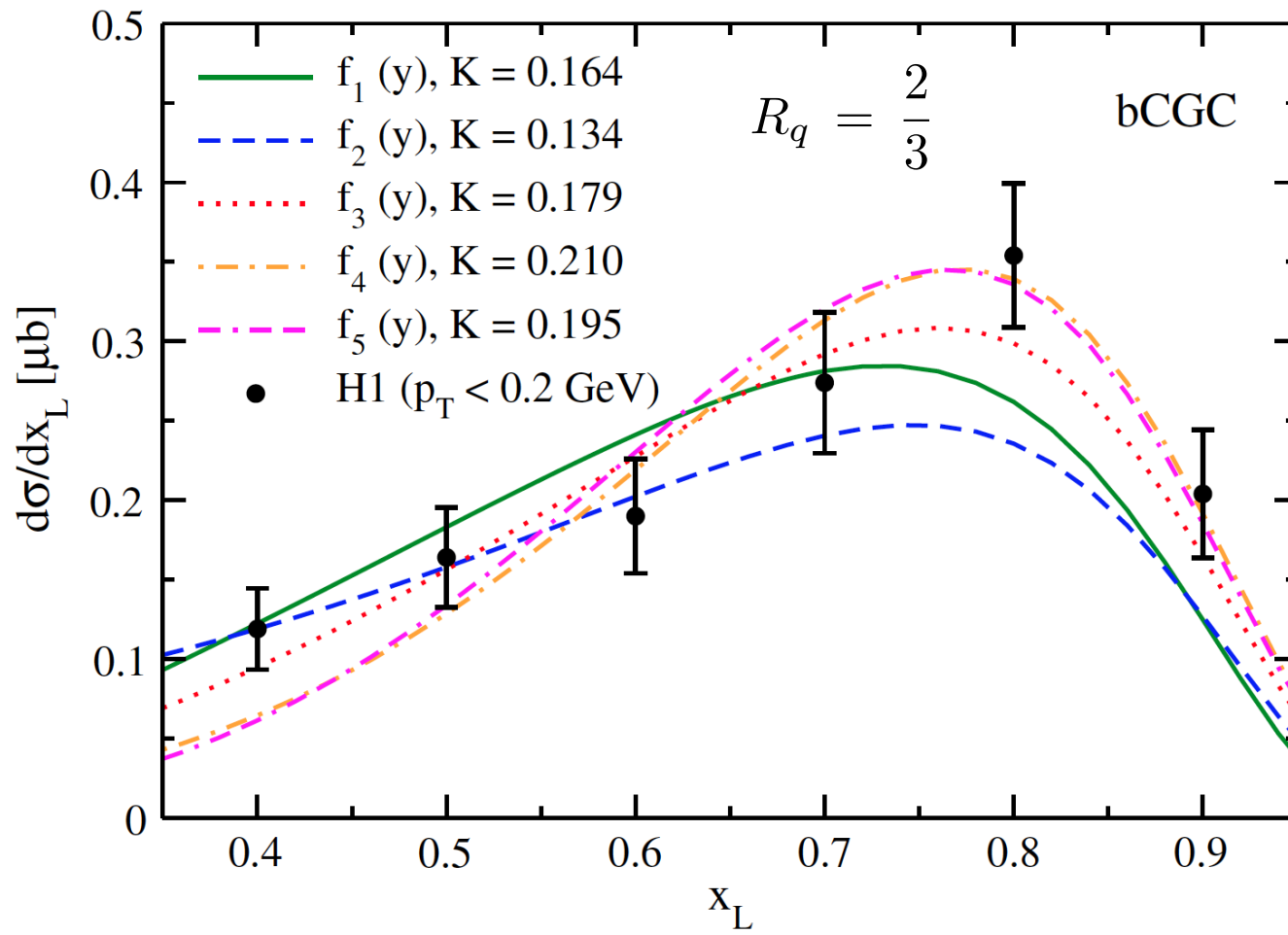
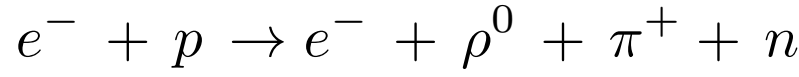
$$(\Psi_V^* \Psi)_L = \frac{\hat{e}_f e N_c}{4\pi} 2Qz(1-z) K_0(\epsilon r) \left[M_V \phi_L(r, z) + \delta \frac{m_f^2 - \nabla_r^2}{M_V z(1-z)} \phi_L(r, z) \right]$$

boosted Gaussian

$$\left\{ \begin{array}{l} \phi_{T,L}(r, z) = \mathcal{C}_{T,L} z(1-z) \exp \left[-\frac{m_f^2 R^2}{8z(1-z)} - \frac{2z(1-z)r^2}{R^2} + \frac{m_f^2 R^2}{2} \right] \end{array} \right.$$

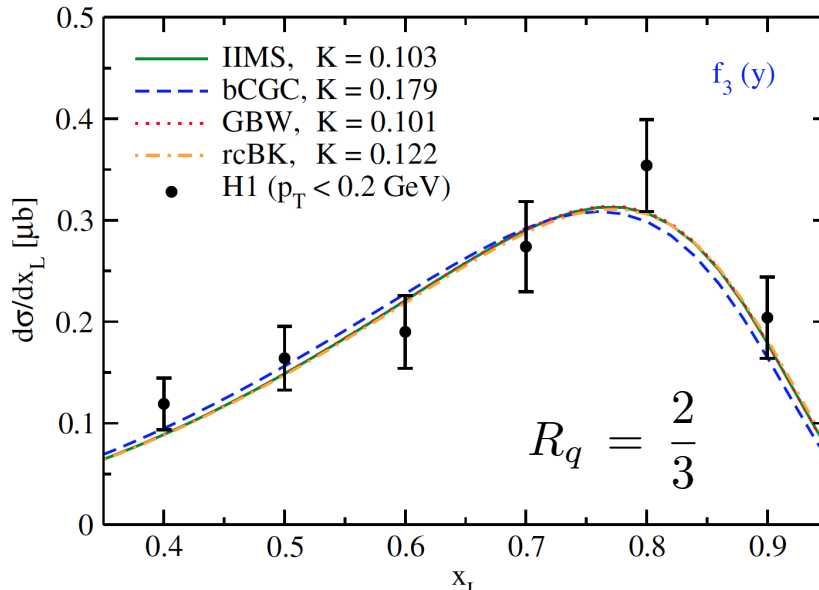
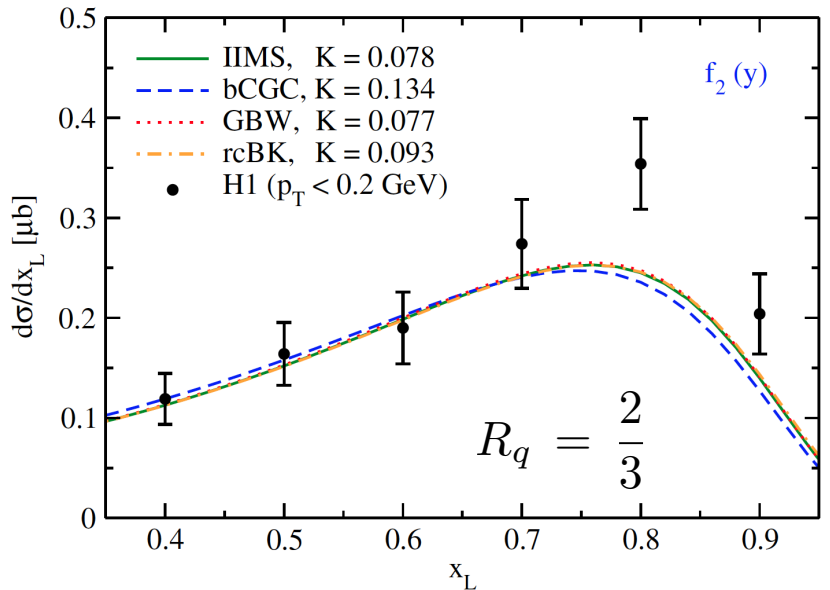
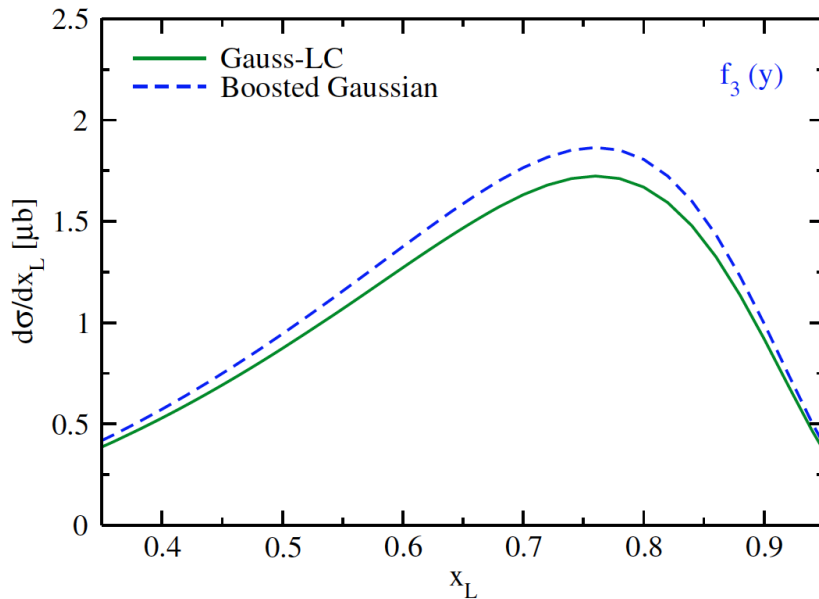
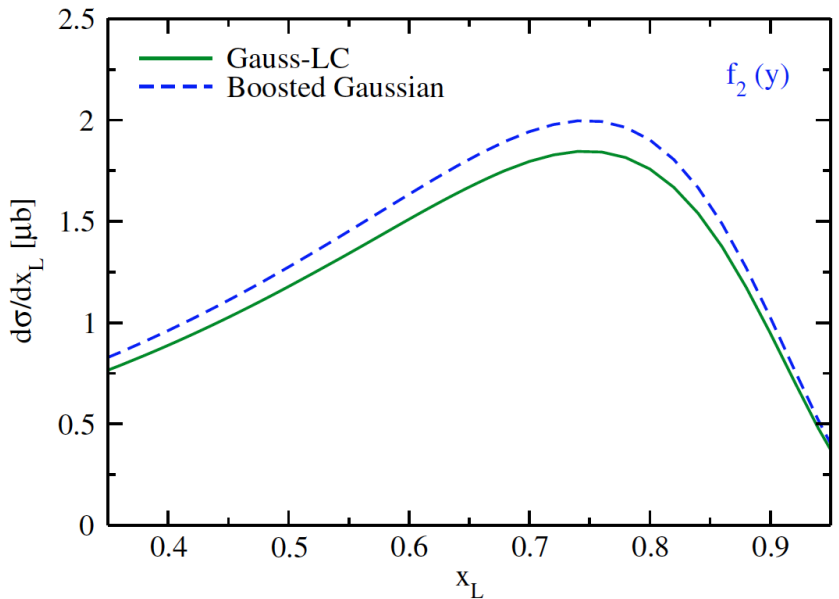
Gauss LC

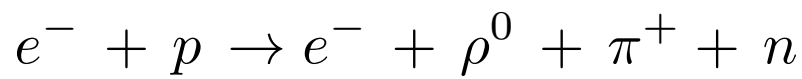
$$\left\{ \begin{array}{l} \phi_T(r, z) = N_T [z(1-z)]^2 \exp(-r^2/2R_T^2) \\ \phi_L(r, z) = N_L z(1-z) \exp(-r^2/2R_L^2) \end{array} \right.$$



H1: V. Andreev et al., EJPC 76, 41 (2016)

Gonçalves, FSN, Spiering, PRD 93 (2016) 054025





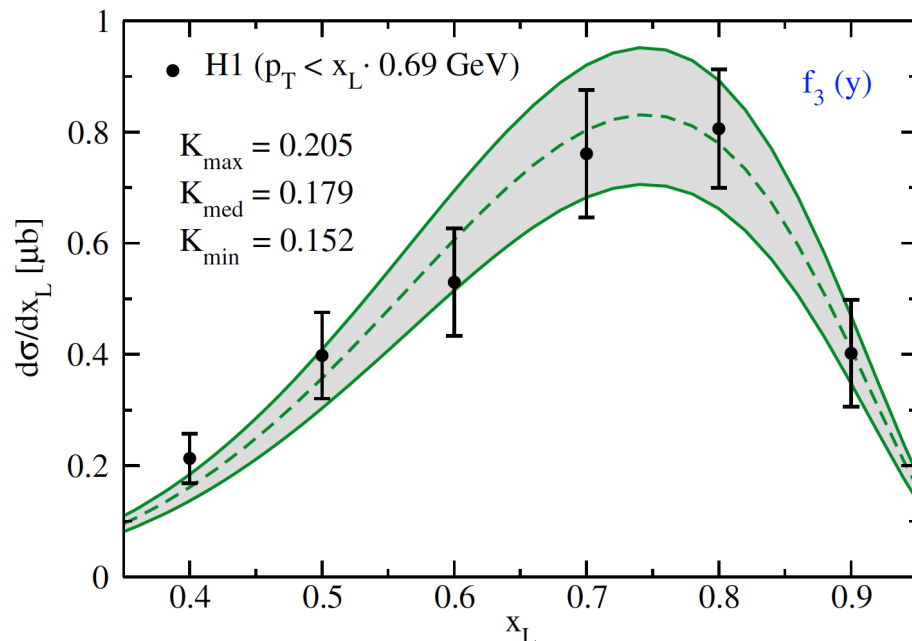
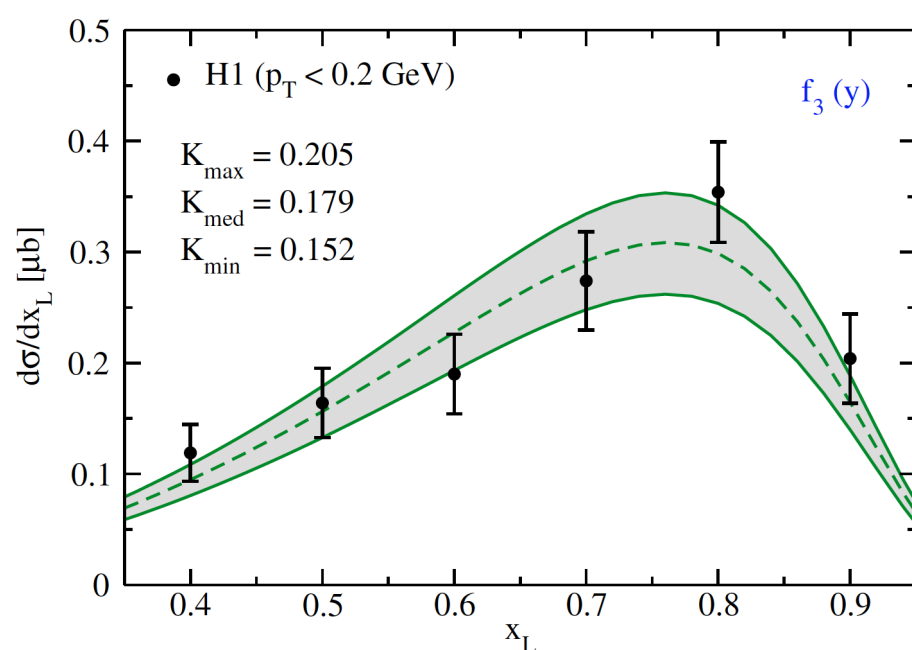
$$R_q = \frac{2}{3}$$

Gauss-LC

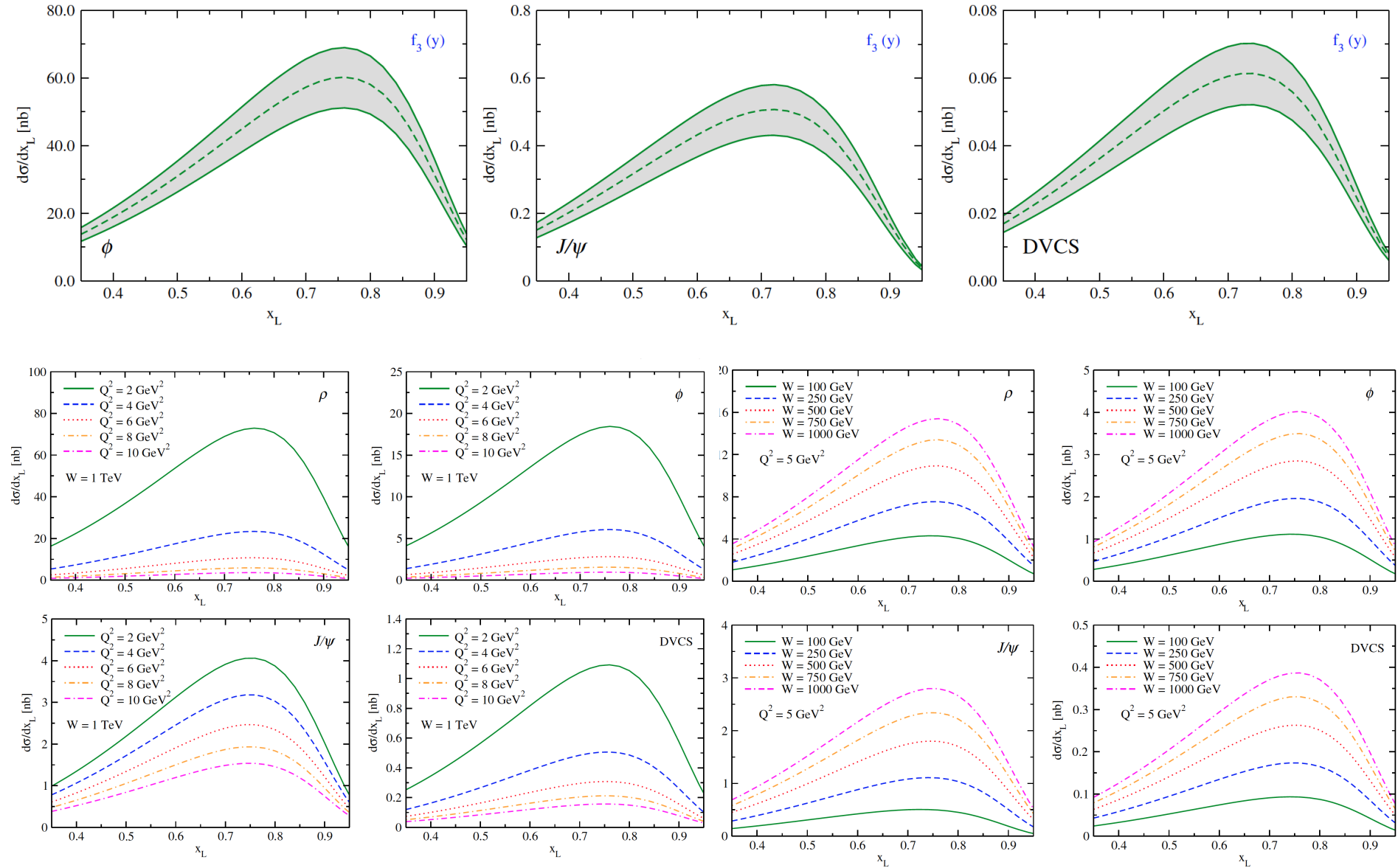
bCGC

$Q^2 = 0.04 \text{ GeV}^2$

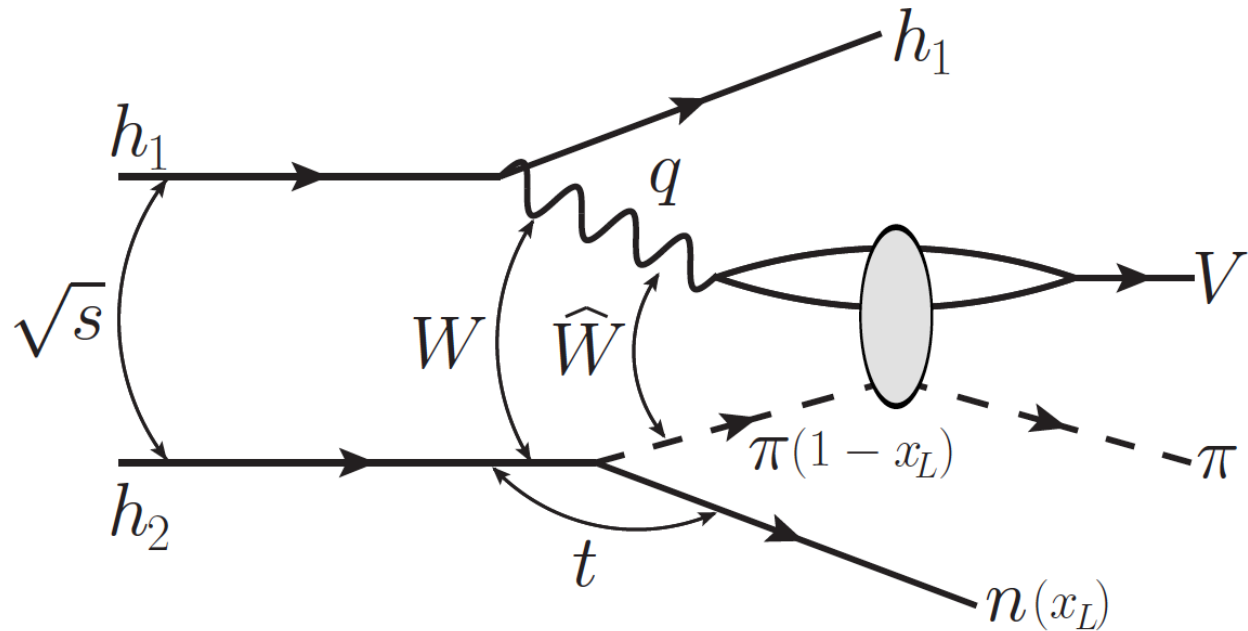
Gonçalves, FSN, Spiering,
PRD 93 (2016) 054025



Predictions



$$p + p \rightarrow p + \rho^0 + \pi^+ + n$$



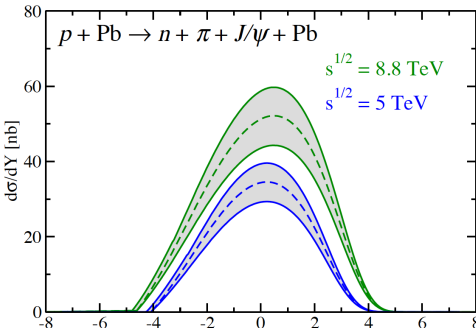
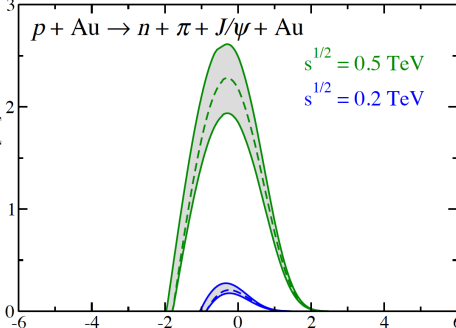
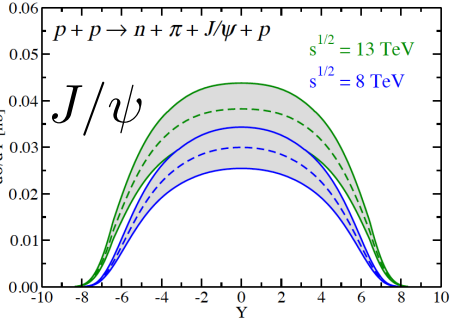
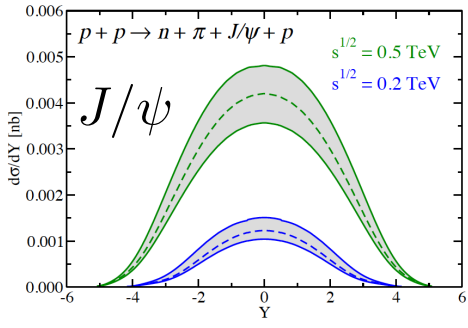
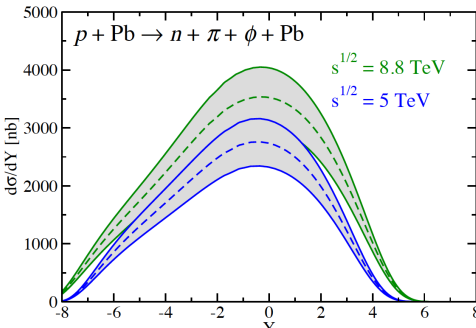
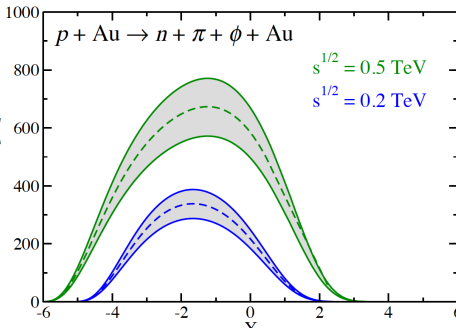
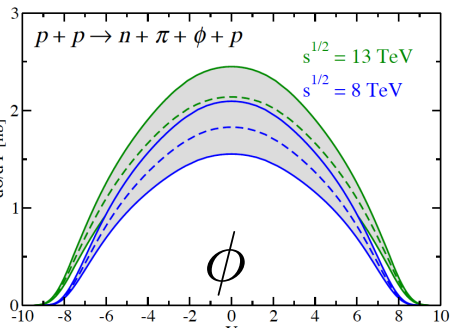
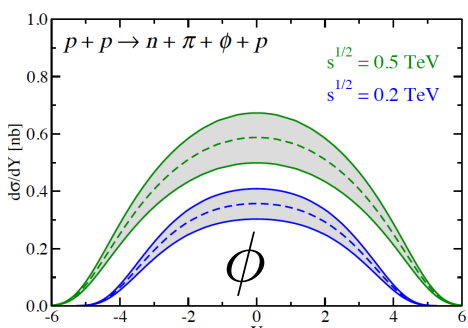
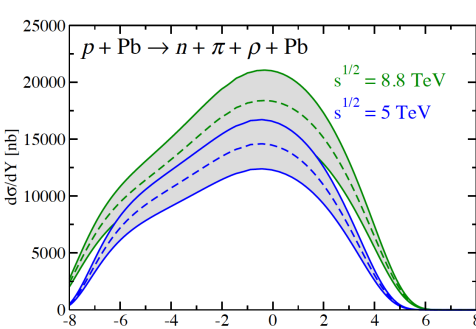
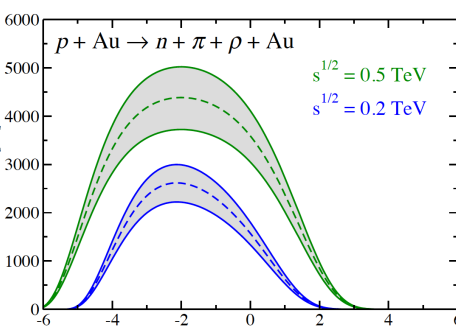
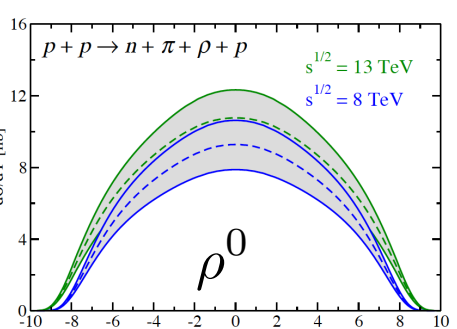
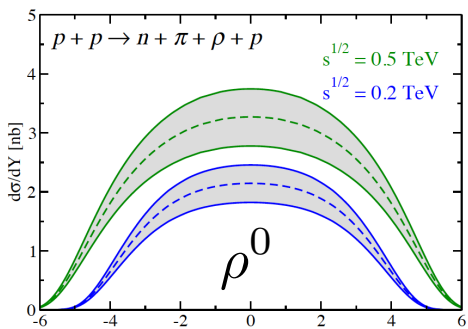
$$R_q = \frac{2}{3} \quad \text{Gauss-LC} \quad \text{bCGC} \quad Q^2 = 0.0 \text{ GeV}^2$$

Gonçalves, Moreira, FSN, Spiering, arXiv:160508186

Predictions

p - p

p - A



Predictions

$\sigma(V)$ [nb]		$\sqrt{s} = 0.2$ TeV	$\sqrt{s} = 0.5$ TeV	$\sqrt{s} = 8.0$ TeV	$\sqrt{s} = 13.0$ TeV
ρ	K_{min}	12.17	22.06	90.12	110.51
	K_{med}	14.34	25.98	106.12	130.14
	K_{max}	16.42	29.75	121.54	149.04
ϕ	K_{min}	1.83	3.58	16.67	20.73
	K_{med}	2.15	4.21	19.63	24.42
	K_{max}	2.46	4.83	22.48	27.96
J/ψ	K_{min}	0.0042	0.019	0.25	0.35
	K_{med}	0.0049	0.022	0.30	0.42
	K_{max}	0.0064	0.026	0.34	0.48

p - p

$\sigma(V)$ [nb]		$\sqrt{s} = 0.2$ TeV	$\sqrt{s} = 0.5$ TeV	$\sqrt{s} = 5.0$ TeV	$\sqrt{s} = 8.8$ TeV
ρ	K_{min}	9176.88	20819.90	102785.00	139110.00
	K_{med}	10807.00	24518.30	121043.00	163821.00
	K_{max}	12376.70	28079.50	138625.00	187616.00
ϕ	K_{min}	1090.55	2863.67	17326.20	24154.90
	K_{med}	1278.41	3386.65	20403.80	28445.60
	K_{max}	1470.81	3862.20	23367.50	32577.30
J/ψ	K_{min}	0.19	3.94	135.53	234.50
	K_{med}	0.23	4.65	159.61	276.16
	K_{max}	0.32	5.65	184.04	317.05

p - A

Summary

LN spectra in the dipole approach: several processes in the same framework

Not included:

{ fragmentation
 $\Delta^+ \rightarrow \pi^+ n$ (small contribution or only at low x_L)
 ρ exchange

Uncertainties:

{ "additive quark model" $\frac{1}{3} < R_q < \frac{2}{3}$
absorption $0.5 < K < 1$
pion flux
dipole cross section
vector meson wave function

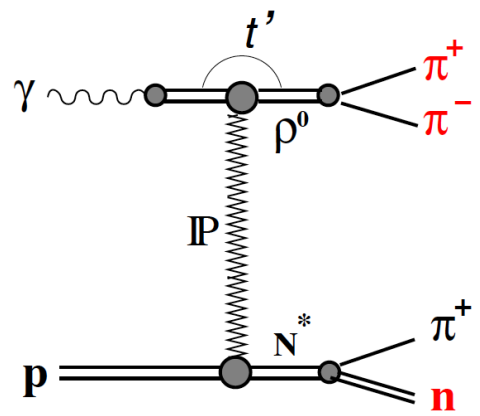
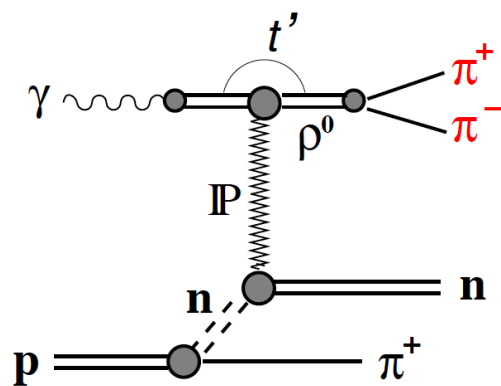
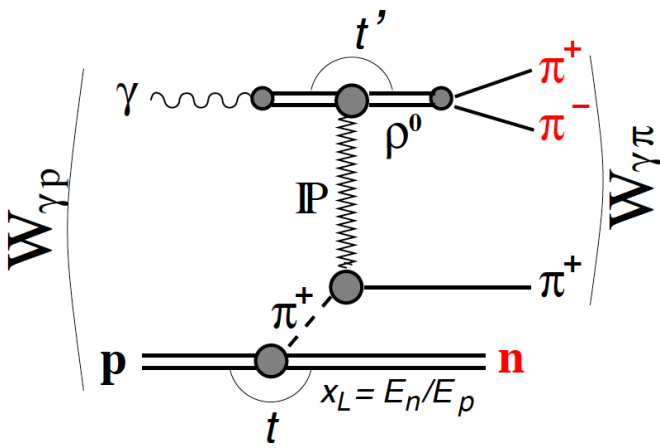
To improve: data on LN with dijet production, charm production,...

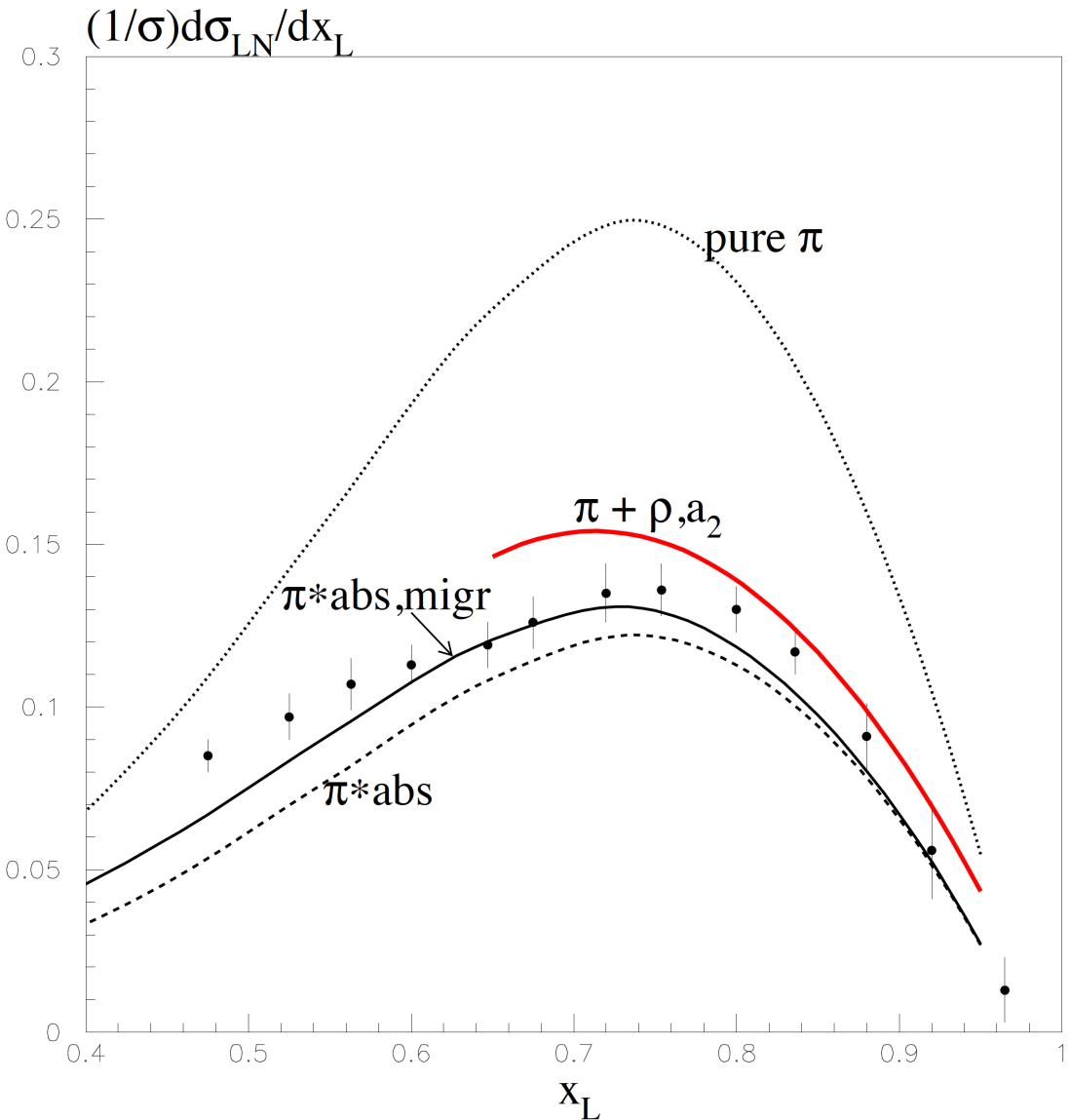
Extension to pp and pA



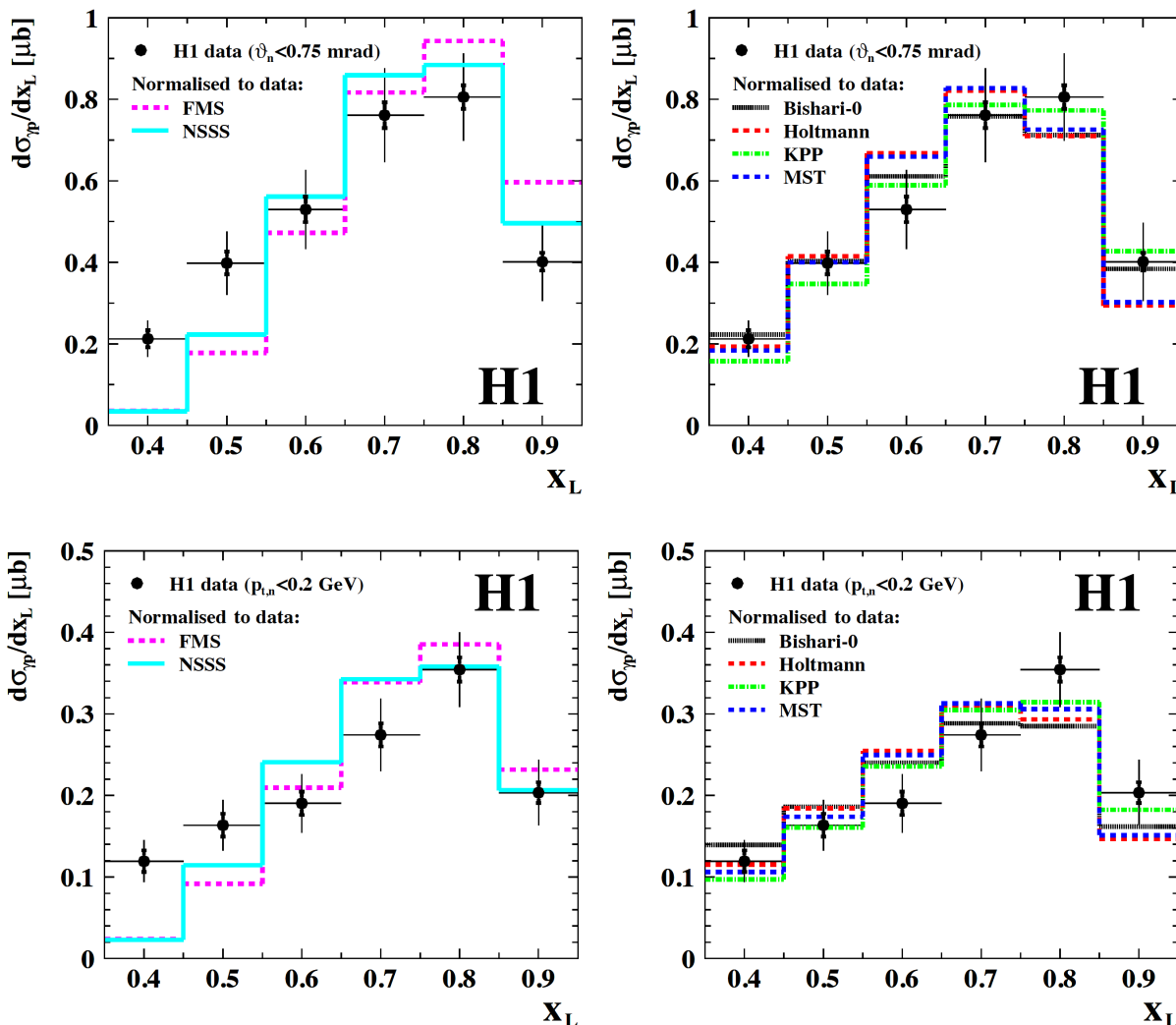
Thank you !

Back ups





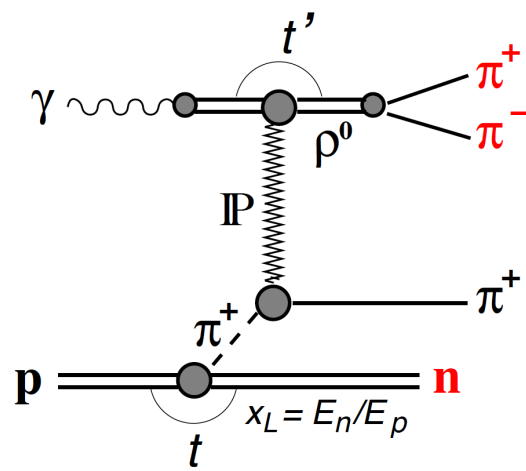
ρ^0 with Forward Neutron



H1: V. Andreev et al., EJPC 76, 41 (2016)

Energy dependence and Feynman scaling

Kaidalov, Khose, Martin, Ryskin, hep-ph/0602215



$$\frac{d^2\sigma(W,Q^2,x_L,t)}{dx_Ldt} = f_{\pi/p}(x_L,t) \underline{\sigma_{\gamma^*\pi}(\hat{W}^2,Q^2)}$$

$$\underline{\sigma_{\gamma^*\pi}(\hat{x},Q^2)} = \frac{2}{3}\sigma_{\gamma^*p}(\hat{x},Q^2) = \frac{2}{3}\int_0^1 dz \int d^2r \sum_{L,T} |\Psi_{T,L}(z,r,Q^2)|^2 \underline{\sigma_{dip}(\hat{x},r)}$$

$$\underline{\sigma_{dip}(r,\hat{x})} = 2 \int d^2\mathbf{b} \mathcal{N}(r,\hat{x},\mathbf{b}) = \sigma_0 \ [1 - exp(-\frac{(Q_s(\hat{x})r)^2}{4})]$$

$$Q_s^2(\hat{x})=Q_0^2\left(\frac{x_0}{\hat{x}}\right)^\lambda$$

$$Q_s^2 \rightarrow 0 \quad (\text{low } W)$$

$$\sigma_{dip}(r,\hat{x}) \simeq \sigma_0 \frac{Q_s^2(\hat{x})r^2}{4} \simeq \sigma_0 Q_0^2 x_0^\lambda [\frac{(1-x_L)W^2+Q^2}{Q^2+m_f^2}]^\lambda \quad \text{linear}$$

$$Q_s^2 \rightarrow \text{large} \quad (\text{high } W)$$

$$\sigma_{dip}(r,\hat{x}) = \sigma_0 \mathcal{N}(r,\hat{x}) \simeq \sigma_0 \quad \text{saturation}$$

Future:

TeV electron-proton collider

Paul Newman's talk

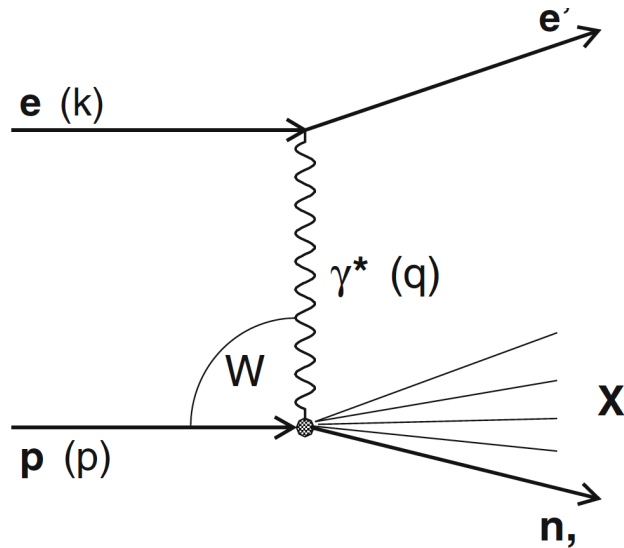
Claire Gwenlan's talk

Very High Energy electron-proton collider (VHEeP)

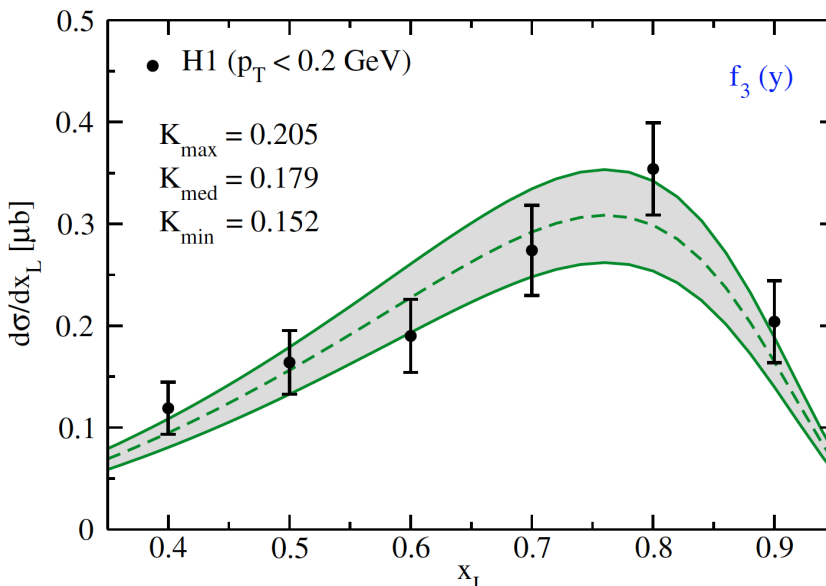
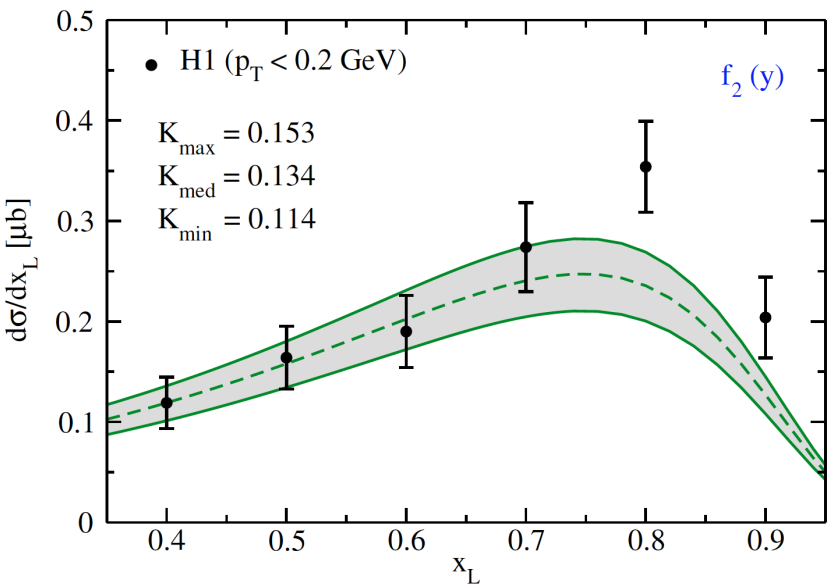
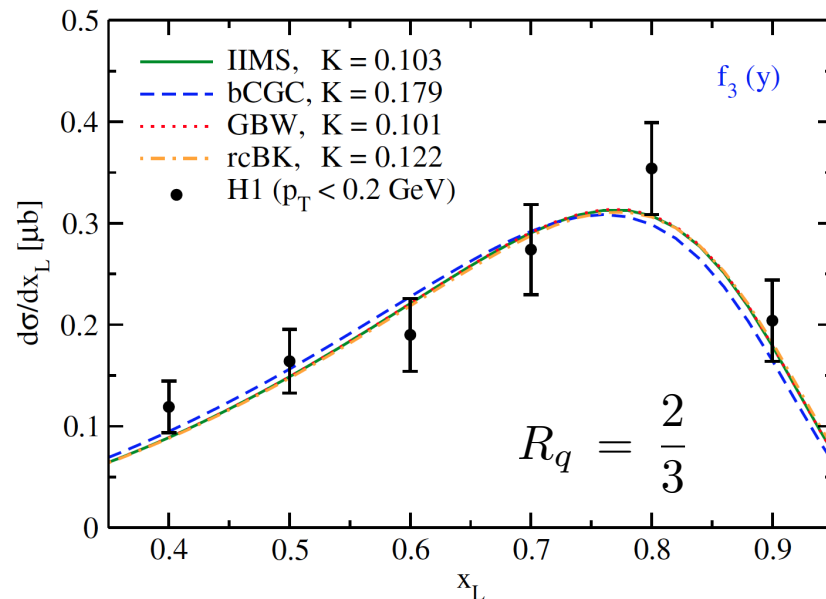
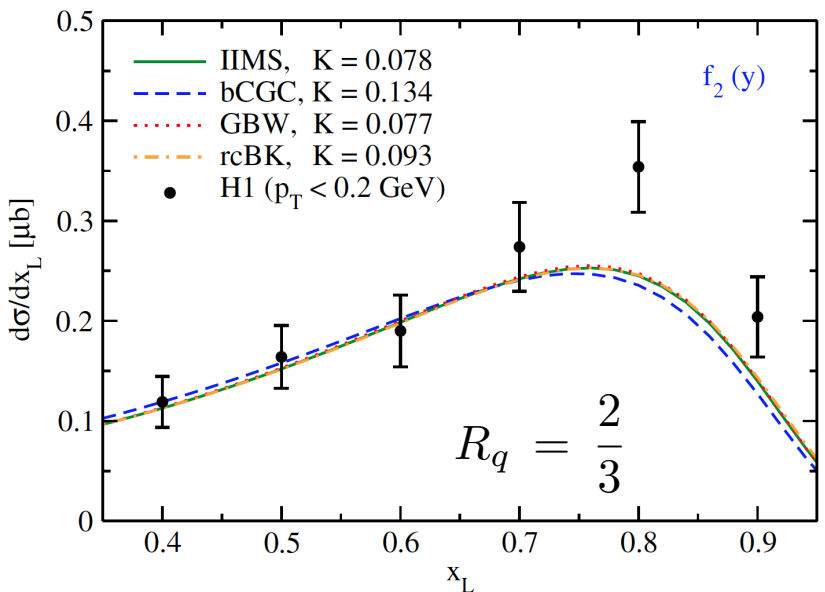
Caldwell, Wing arXiv:1509.00235

Learn more about the pion structure function

Leading neutrons in Deep Inelastic Scattering



normal DIS
with quark fragmentation



$$\frac{d^2\sigma(W,Q^2,x_L,t)}{dx_Ldt}=f_{\pi/p}(x_L,t)\underline{\sigma_{\gamma^*\pi}(\hat W^2,Q^2)}$$

$$\frac{d^2\sigma(W,Q^2,x_L,t)}{dx_Ldt}=f_{\pi/p}(x_L,t)\underline{\sigma_{\gamma^*\pi}(\hat{W}^2,Q^2)}$$

$$\underline{\sigma_{\gamma^*\pi}(\hat{x},Q^2)}=\frac{2}{3}\sigma_{\gamma^*p}(\hat{x},Q^2)=\frac{2}{3}\int_0^1dz\int d^2r\sum_{L,T}|\Psi_{T,L}(z,r,Q^2)|^2\underline{\sigma_{dip}(\hat{x},r)}$$

$$\frac{d^2\sigma(W,Q^2,x_L,t)}{dx_Ldt}=f_{\pi/p}(x_L,t)\underline{\sigma_{\gamma^*\pi}(\hat W^2,Q^2)}$$

$$\underline{\sigma_{\gamma^*\pi}(\hat x,Q^2)}=\frac{2}{3}\sigma_{\gamma^*p}(\hat x,Q^2)=\frac{2}{3}\int_0^1dz\int d^2r\sum_{L,T}|\Psi_{T,L}(z,r,Q^2)|^2\underline{\sigma_{dip}(\hat x,r)}$$

$$\underline{\sigma_{dip}(r,\hat x)}=2\int d^2\boldsymbol b \mathcal N(r,\hat x,\boldsymbol b)=\sigma_0~[1-exp(-\frac{(Q_s(\hat x)r)^2}{4})]$$

$$Q_s^2(\hat x) = Q_0^2 \left(\frac{x_0}{\hat x} \right)^\lambda$$

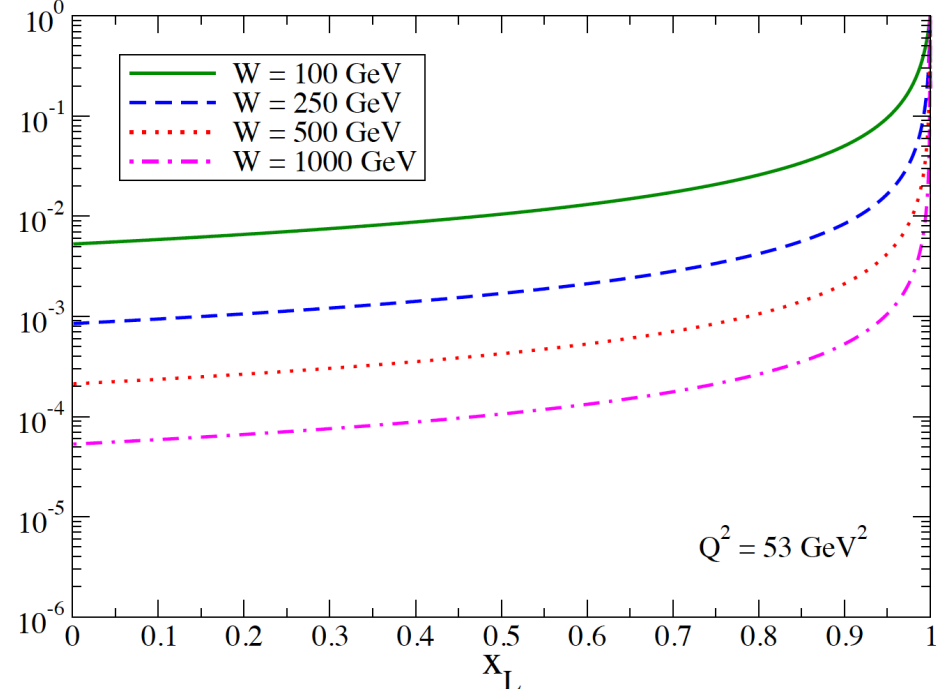
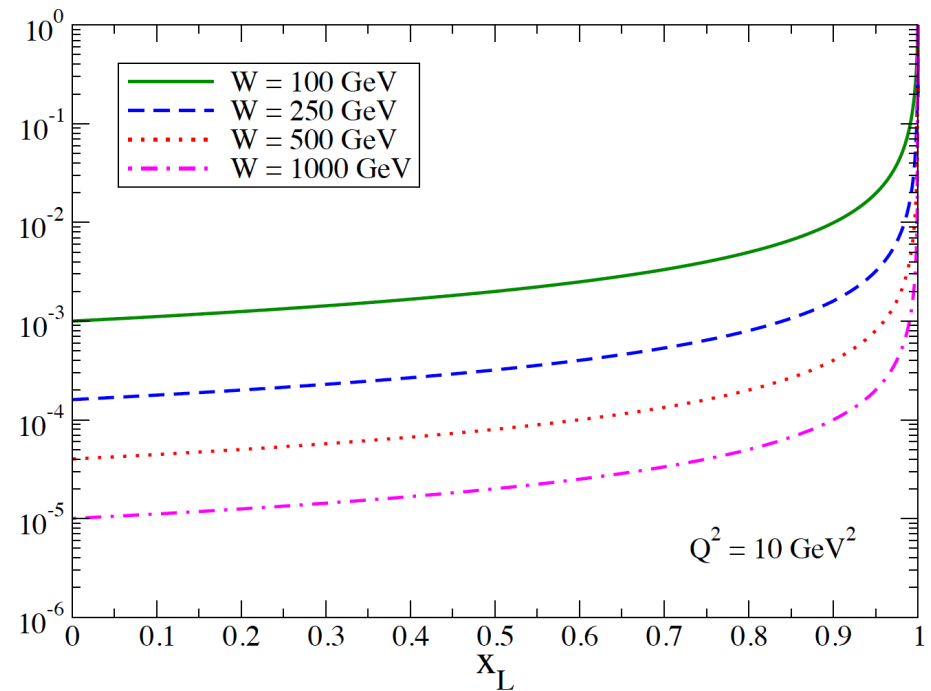
Chiral perturbation theory

$$f_{\pi/p}(y, k_T^2) = \frac{g_A^2 m_p^2}{4\pi f_\pi^2} \int_0^{p_{T\max}^2} dk_t^2 \frac{y(k_t^2 + y^2 m_p^2)}{[k_T^2 + y m_p^2 + (1-y)m_\pi^2]^2}$$

Salamu, Ji, Melnitchouk, Wang, PRL (2015)
Burkardt et al., PRD (2013)

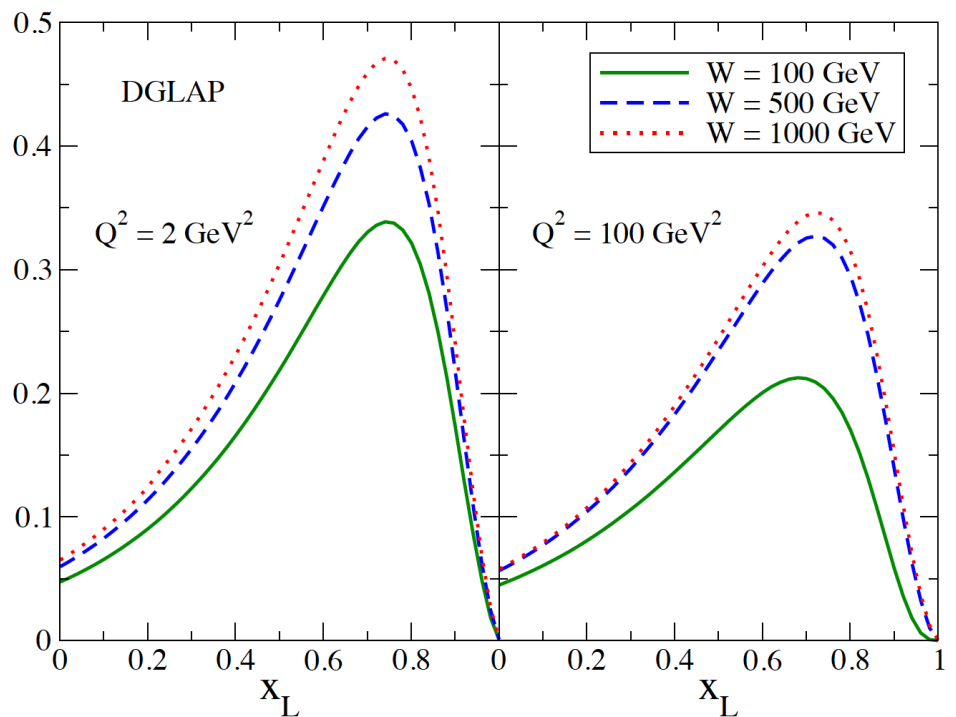
$$\begin{aligned} \mathcal{L}_{\pi N}^{\text{PS}} = -g_{\pi NN} \bar{\psi}_N i \gamma_5 \boldsymbol{\tau} \cdot \boldsymbol{\pi} \psi_N, \quad \xrightarrow{\hspace{1cm}} \quad & \mathcal{L}_{\pi N} = \frac{g_A}{2f_\pi} \bar{\psi}_N \gamma^\mu \gamma_5 \boldsymbol{\tau} \cdot \partial_\mu \boldsymbol{\pi} \psi_N \\ & - \frac{1}{(2f_\pi)^2} \bar{\psi}_N \gamma^\mu \boldsymbol{\tau} \cdot (\boldsymbol{\pi} \times \partial_\mu \boldsymbol{\pi}) \psi_N, \end{aligned}$$

$$\hat{x} = \frac{Q^2 + m_f^2}{\hat{W}^2 + Q^2} = \frac{Q^2 + m_f^2}{(1 - x_L)W^2 + Q^2}$$

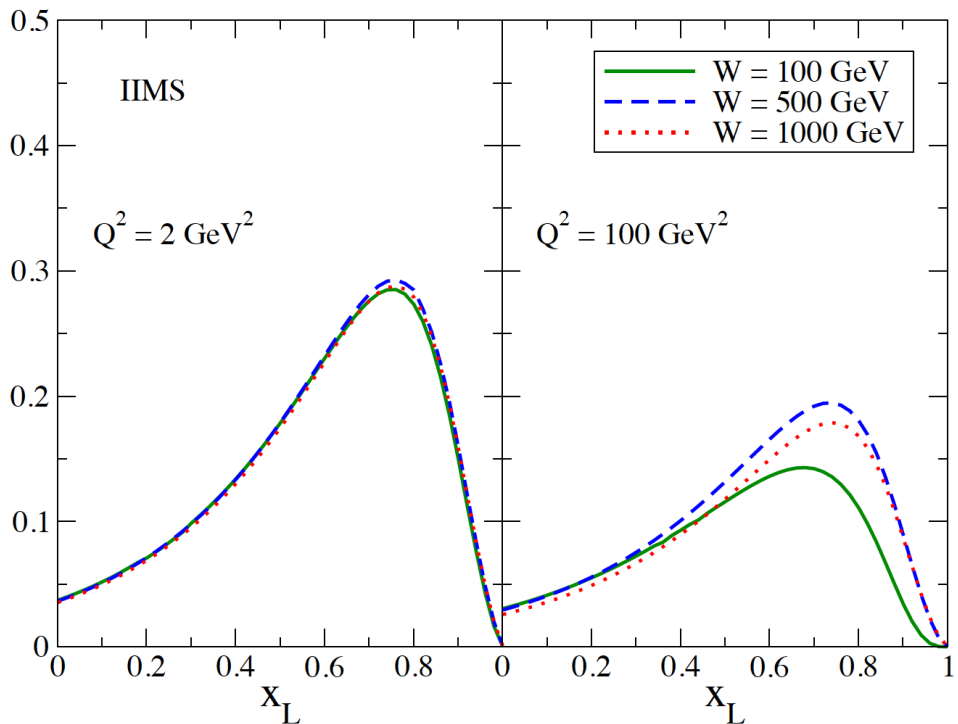


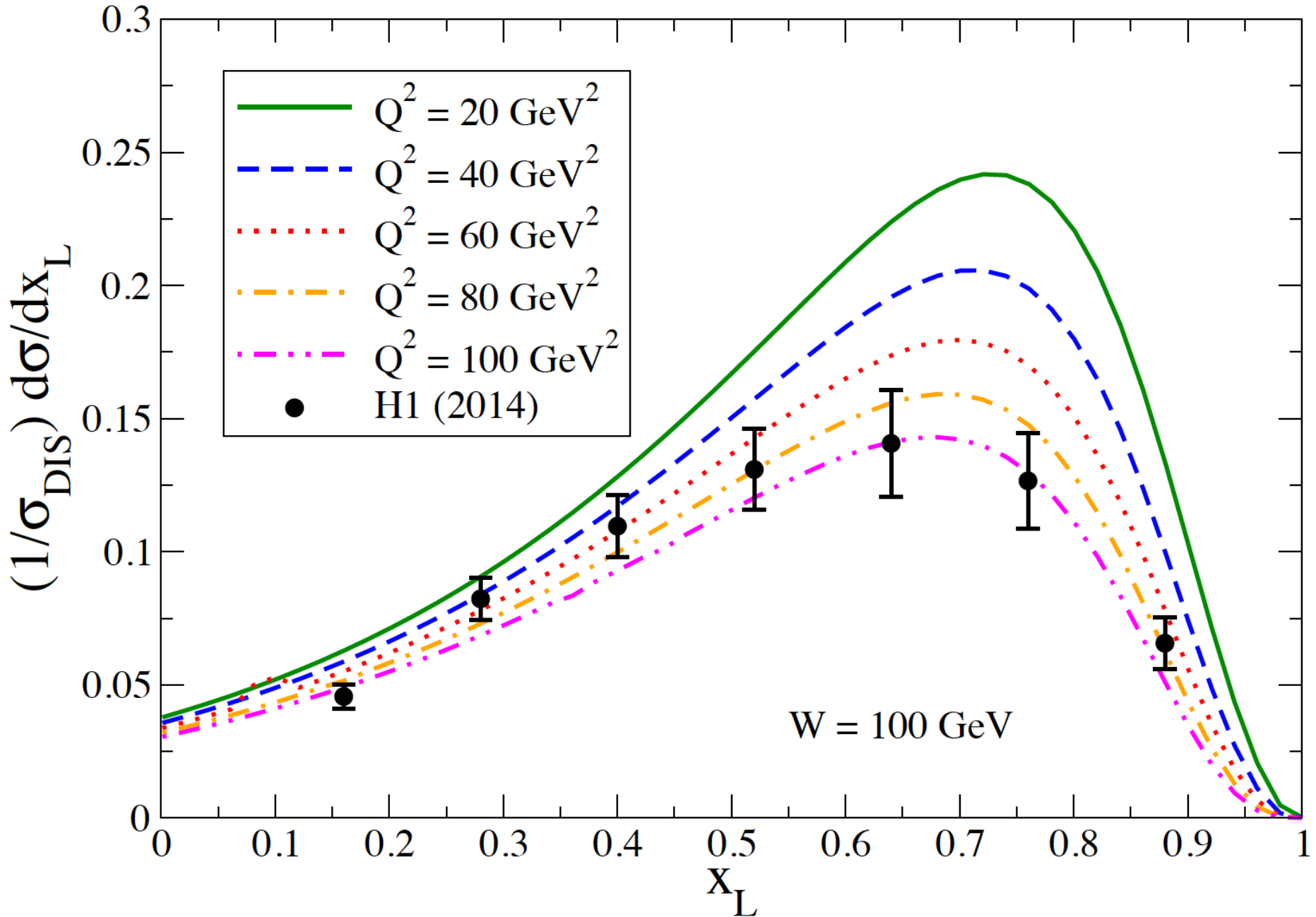
Leading neutron production
can be low x physics !

Linear:

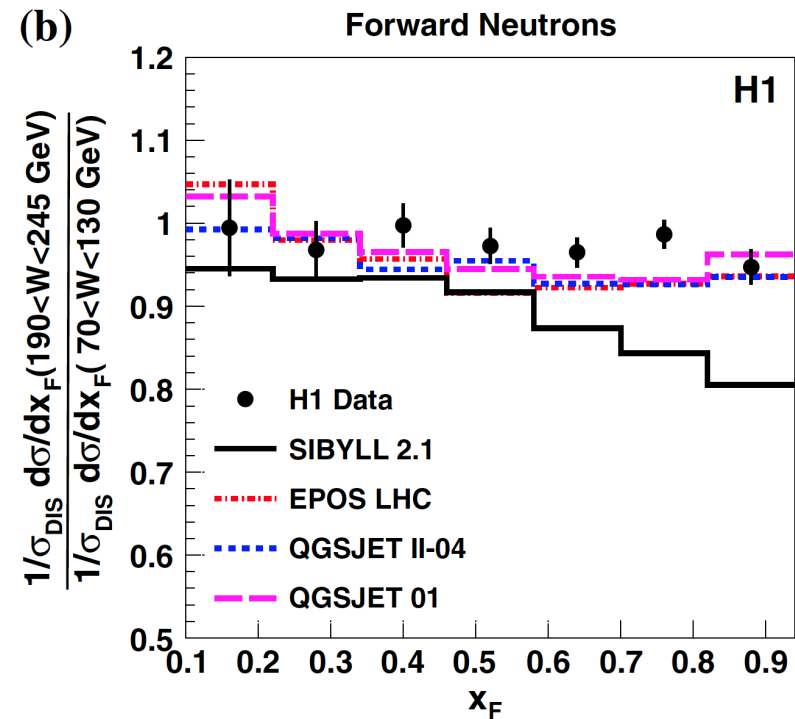
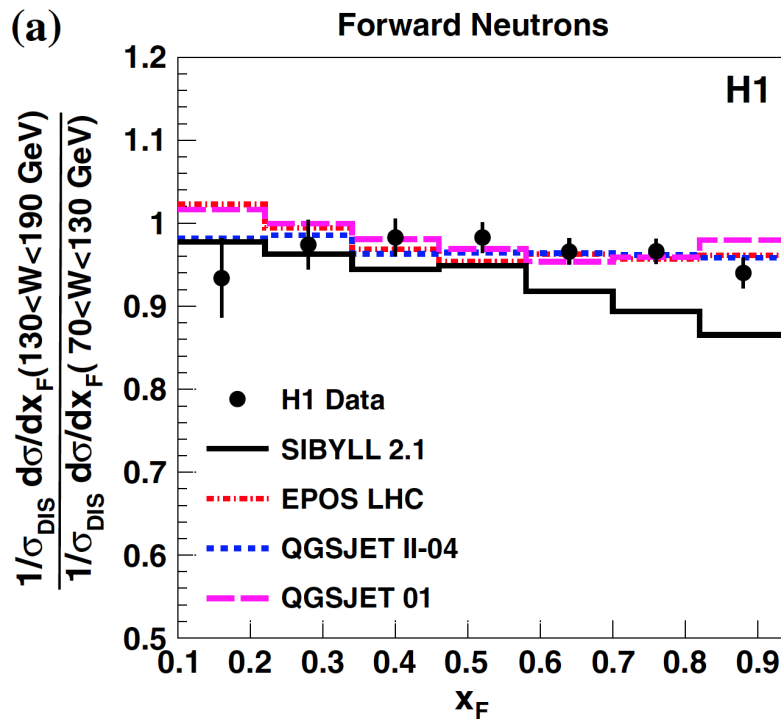


Saturation:





Energy dependence and Feynman scaling



W ranges for cross sections $\frac{1}{\sigma_{DIS}} \frac{d\sigma}{dx_F}$

$70 < W < 130 \text{ GeV}$

$130 < W < 190 \text{ GeV}$

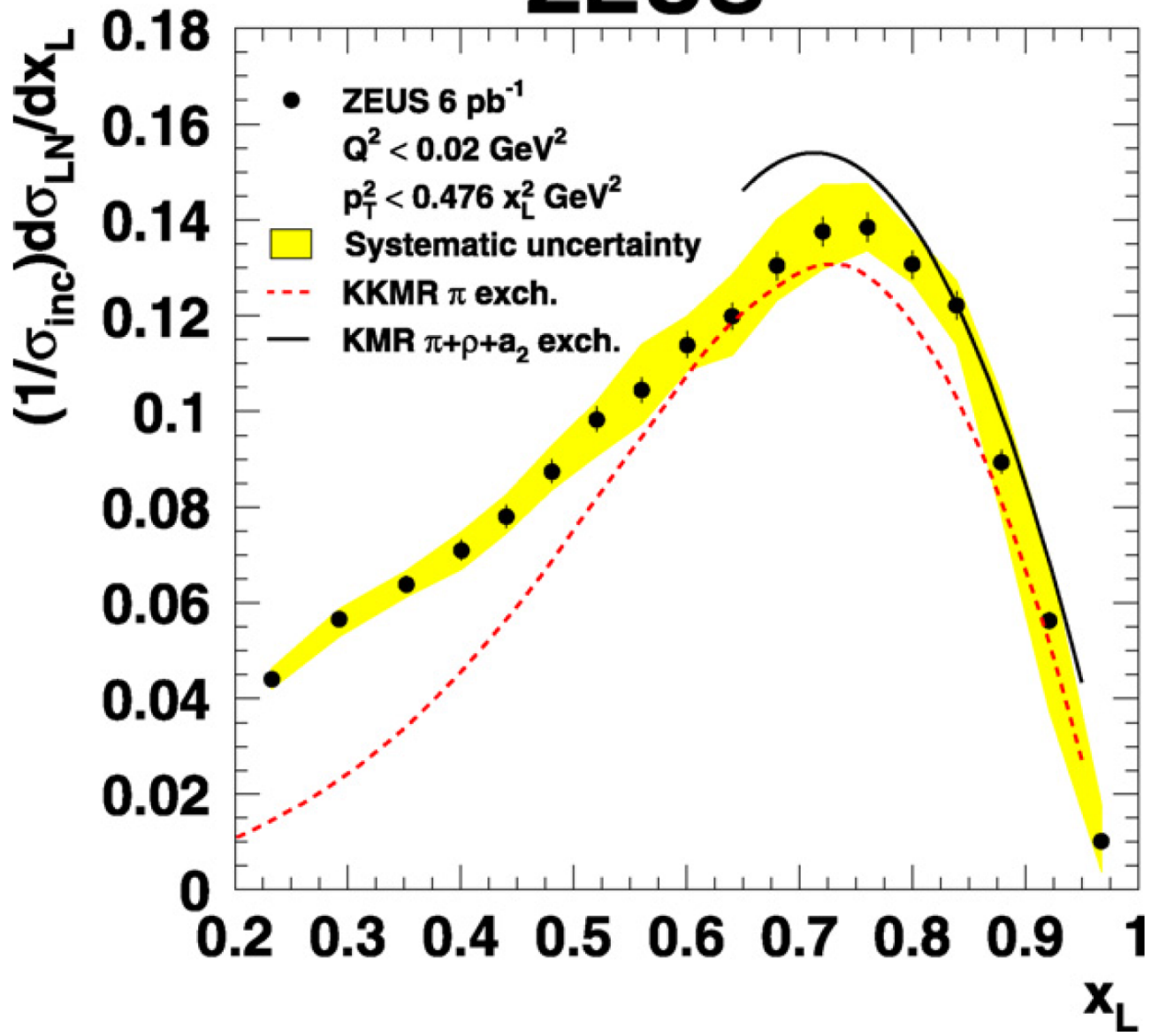
$190 < W < 245 \text{ GeV}$

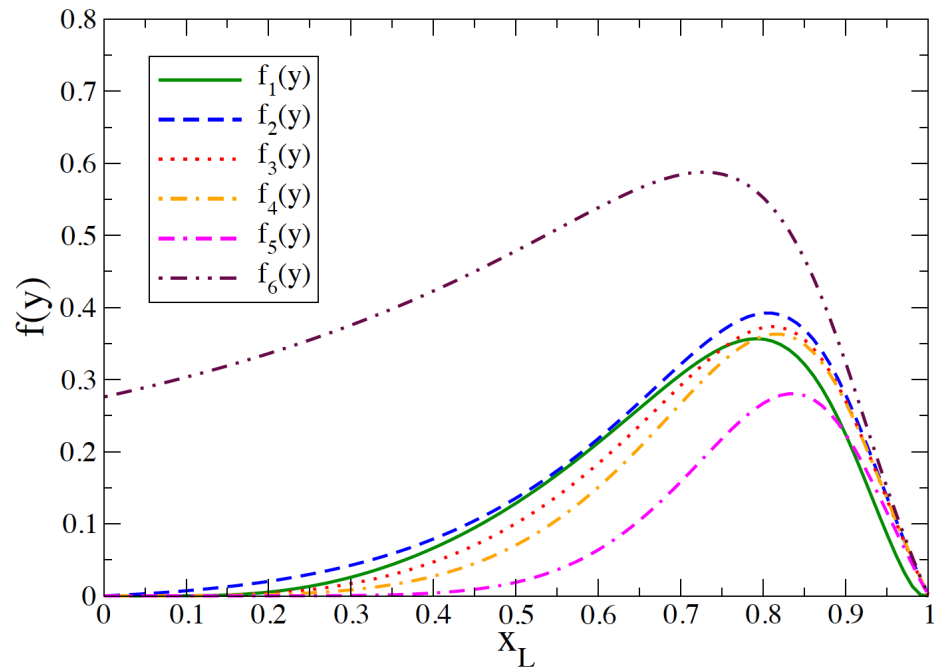
Data from H1 and ZEUS

NC DIS Selection	
$6 < Q^2 < 100 \text{ GeV}^2$	
$0.05 < y < 0.6$	
$70 < W < 245 \text{ GeV}$	
Forward photons	Forward neutrons
$\eta > 7.9$	$\eta > 7.9$
$0.1 < x_F < 0.7$	$0.1 < x_F < 0.94$
$0 < p_T^* < 0.4 \text{ GeV}$	$0 < p_T^* < 0.6 \text{ GeV}$
W ranges for cross sections $\frac{1}{\sigma_{DIS}} \frac{d\sigma}{dx_F}$	
$70 < W < 130 \text{ GeV}$	
$130 < W < 190 \text{ GeV}$	
$190 < W < 245 \text{ GeV}$	

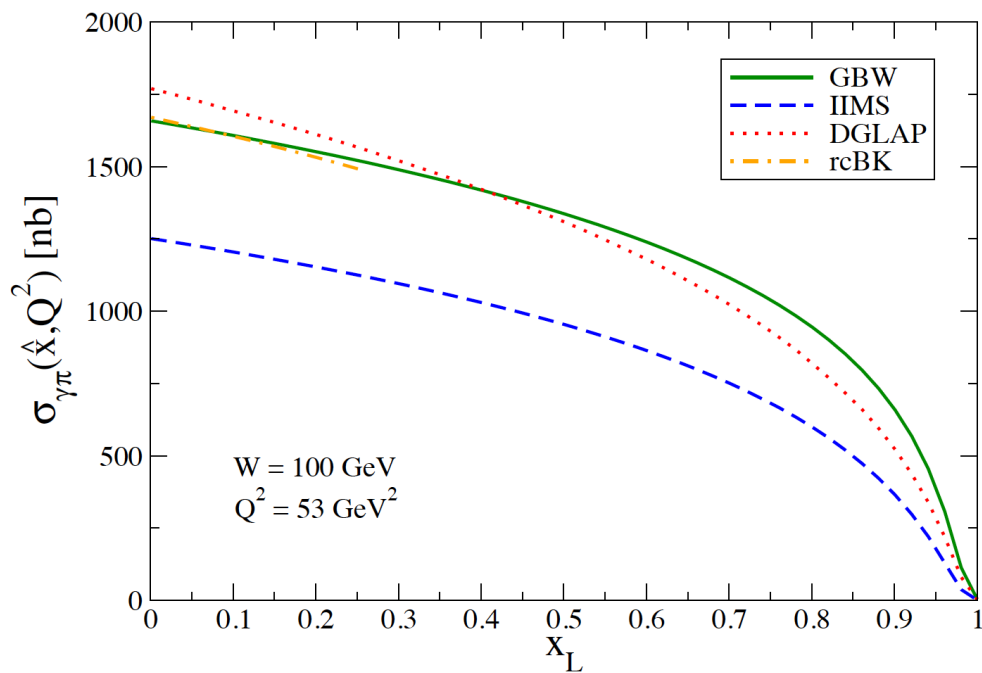
imaginary part of the forward amplitude for the scattering

ZEUS

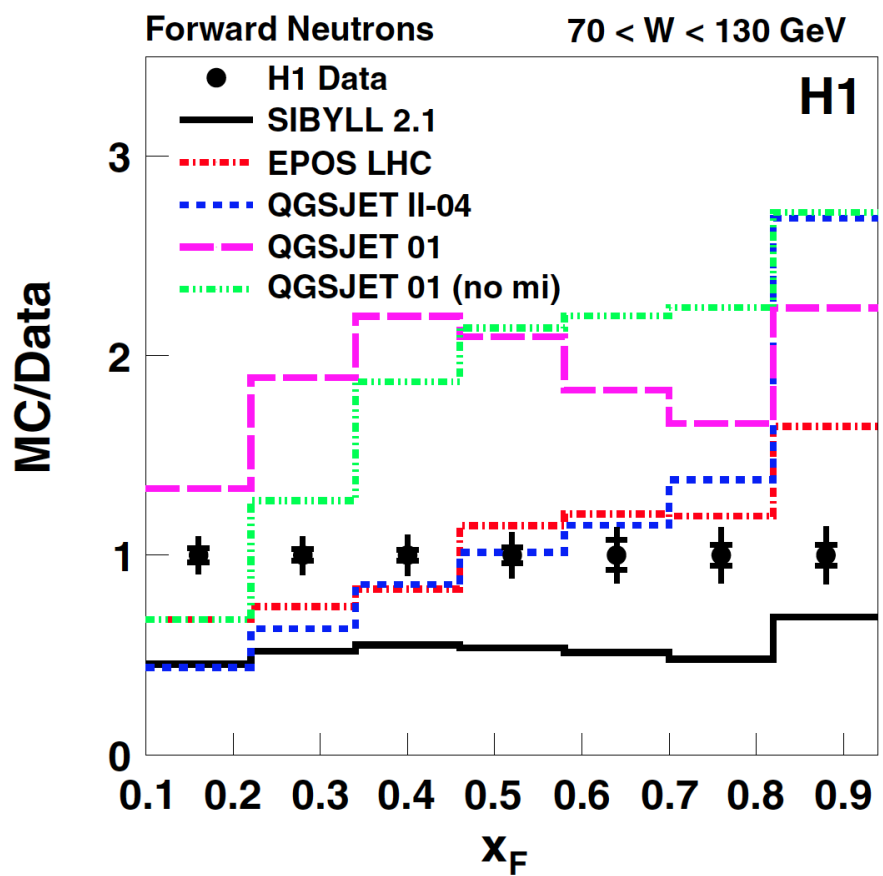
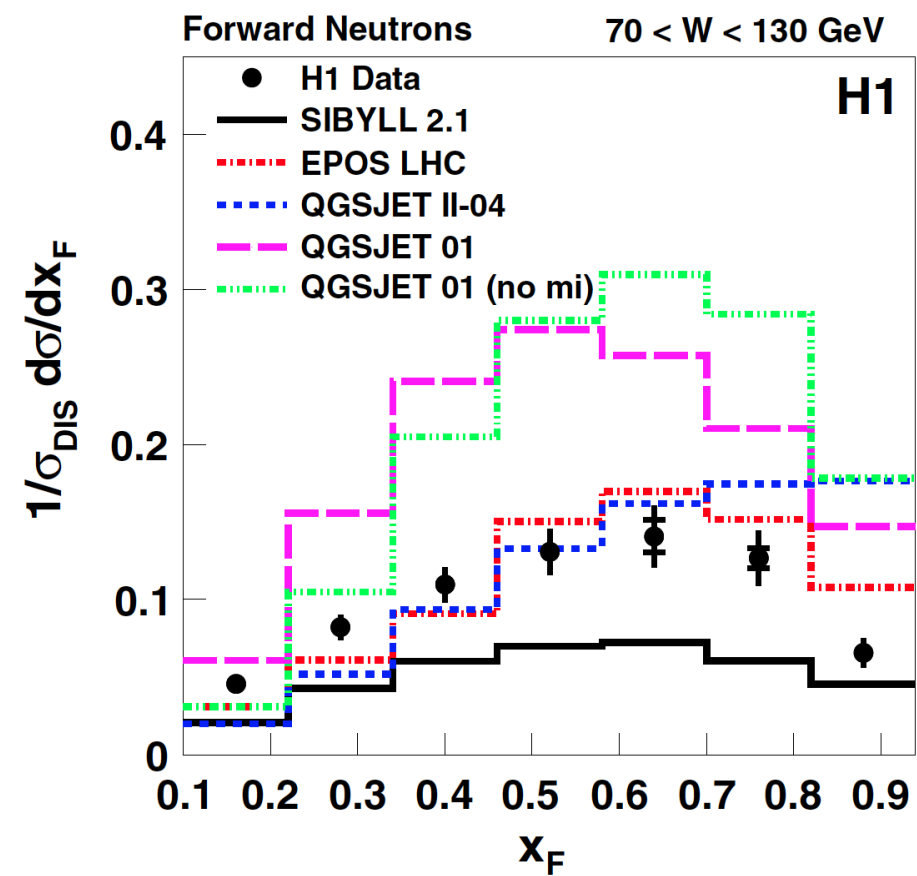




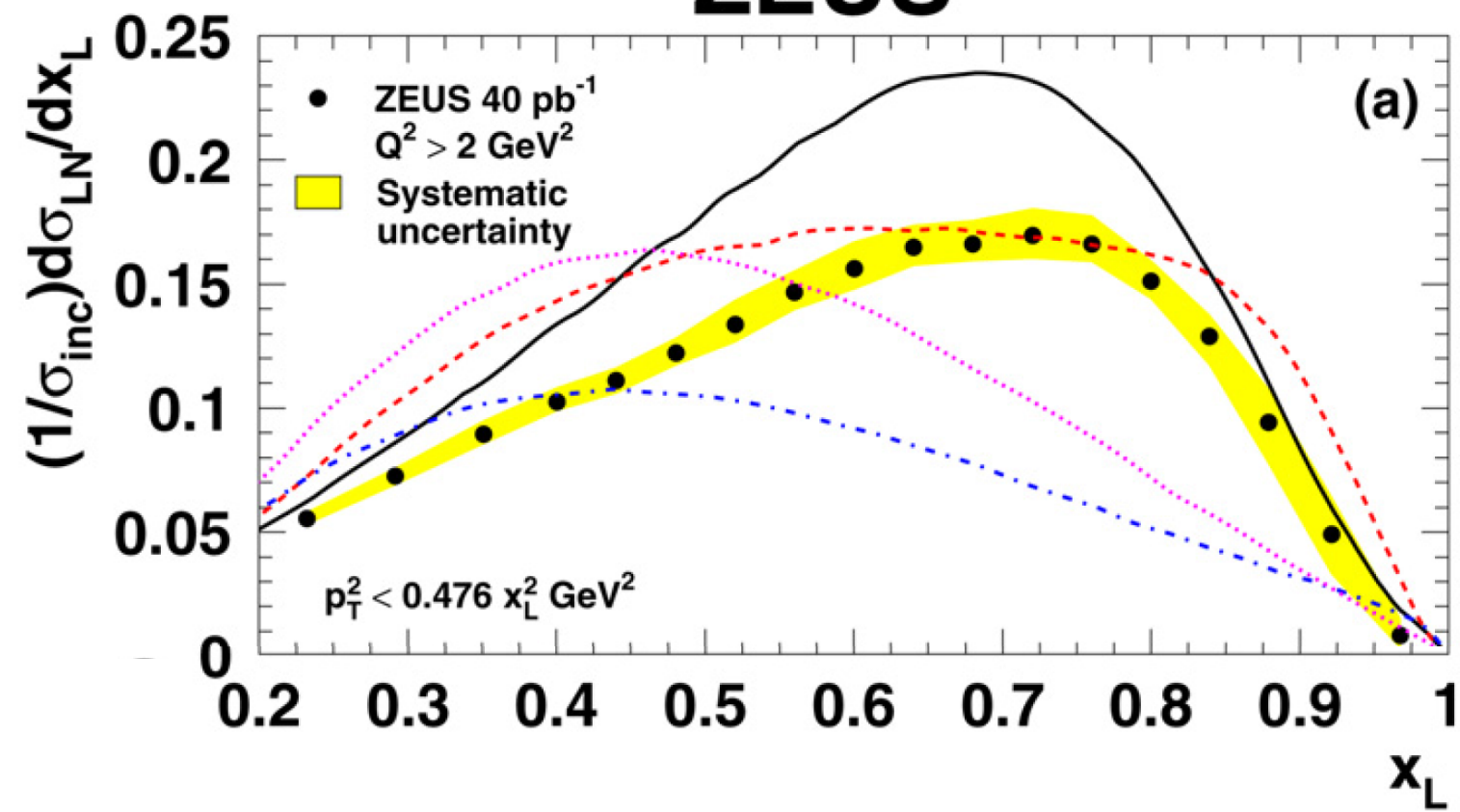
Flux factor

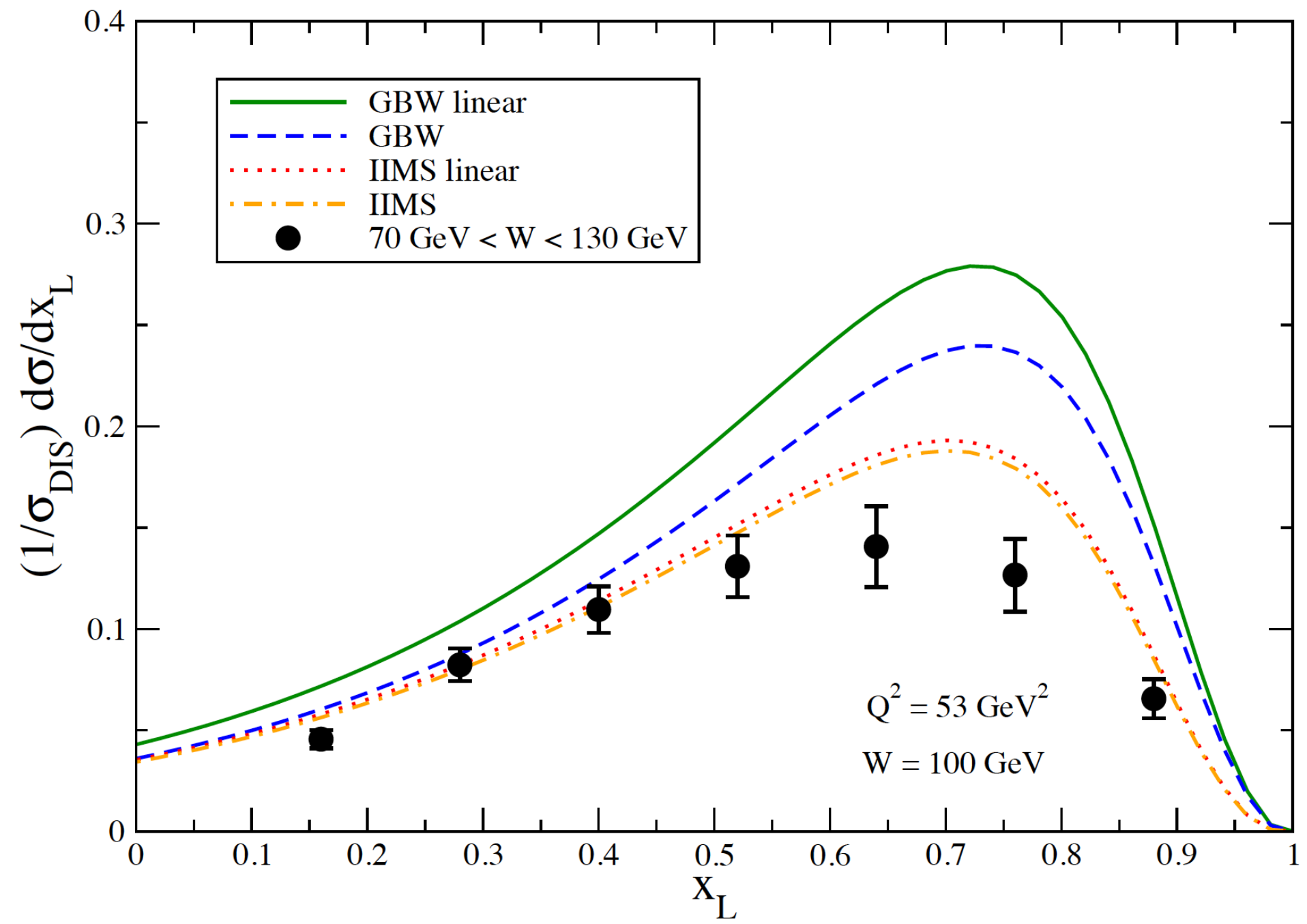


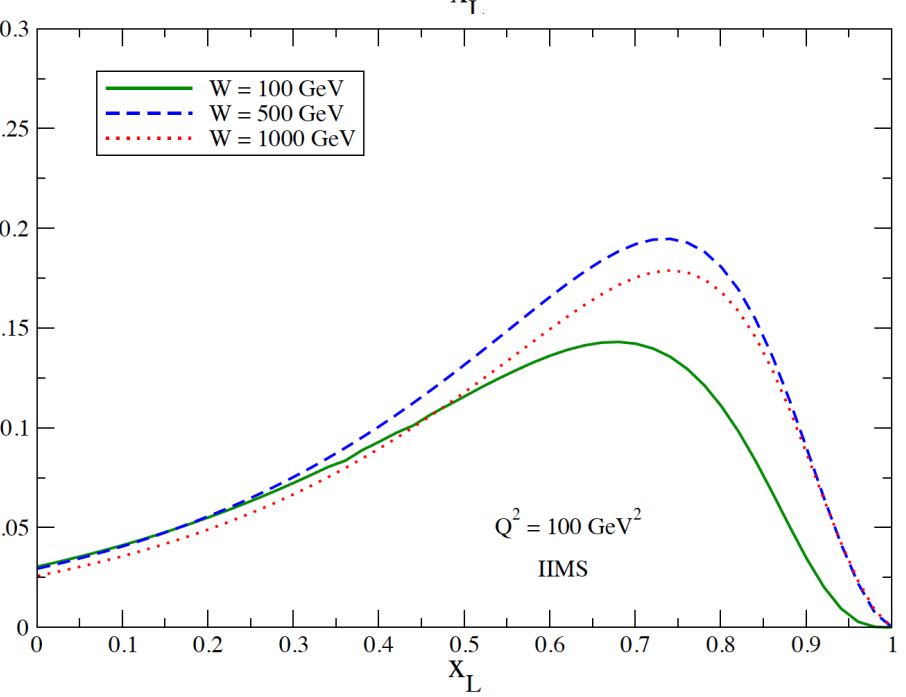
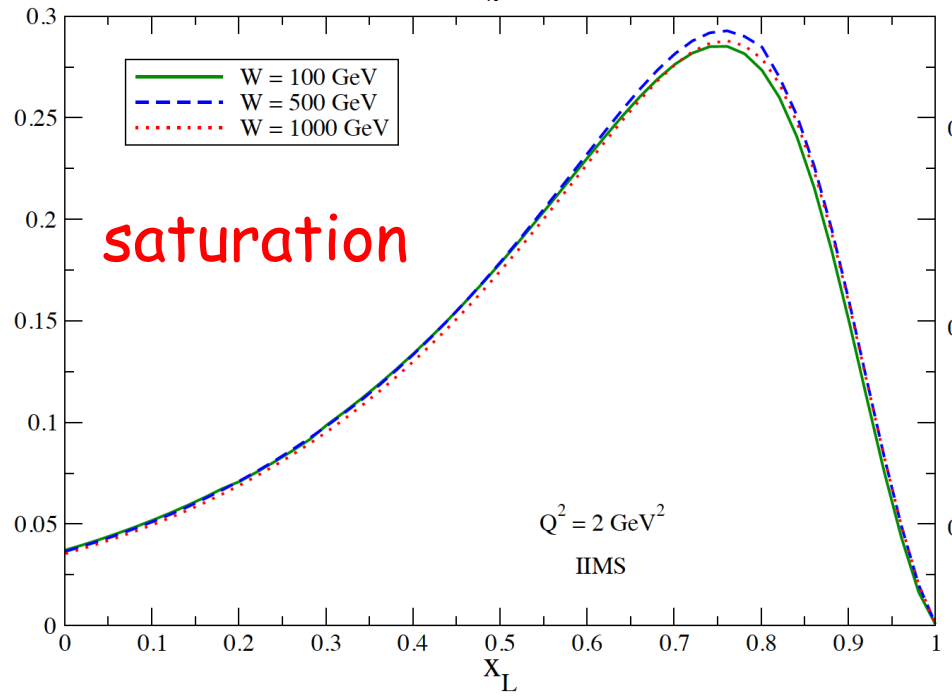
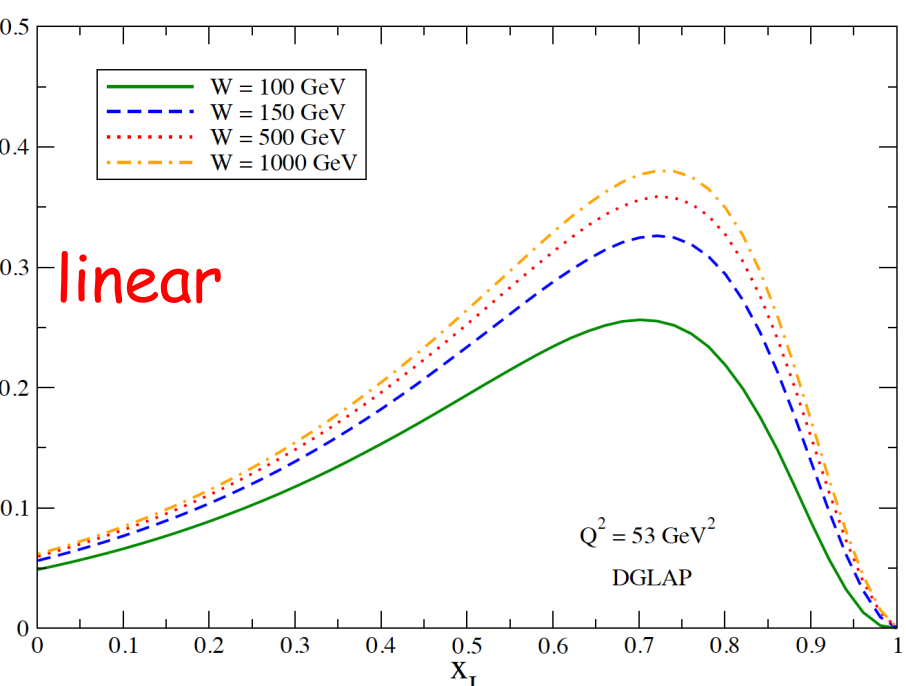
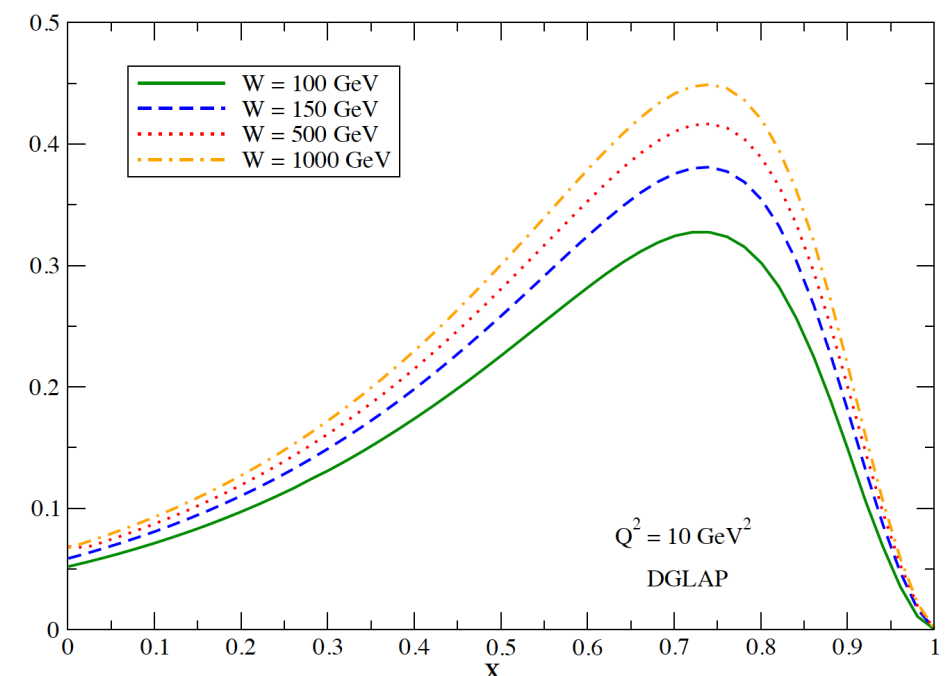
Dipole cross section



ZEUS







Other isovector meson exchanges, such as the ρ or a_2 , can also contribute to direct neutron production. Recent theoretical studies of neutron production in ep collisions show that processes other than direct pion exchange are expected to contribute $\lesssim 25\%$ of neutron production [33, 60, 61, 67]. These backgrounds to OPE, which increase the rate of neutron production in the FNC phase space, are offset by absorptive rescattering of the neutron, which decreases the rate by approximately the amount of the increase [68, 69]. Also absorptive rescattering preferentially removes neutrons with larger p_T , increasing the pion contribution relative to the ρ and a_2 . Therefore these effects are also neglected in the present analysis.

10.1 Competing processes to OPE

Several processes which compete with pion exchange as the mechanism for leading neutron production were ignored in Eq. (16), namely:

- diffractive dissociation in which the dissociated system decays to a state including a neutron

Diffractively produced events can be selected by requiring the presence of a large rapidity gap in the hadronic final state. For such events, the mass of the dissociated proton system is restricted to low values, $M_N \lesssim 4$ GeV.

An event is said to have a large rapidity gap (LRG) in the ZEUS detector if the pseudo-rapidity of the most-forward energy deposit with energy greater than 400 MeV (η_{\max}) is less than 1.8 [64]. Figure 17(a) shows the η_{\max} distributions for both the neutron-tagged and inclusive DIS samples, where the latter has been normalised to the neutron-tagged sample for $\eta_{\max} > 1.8$. For both $\eta_{\max} < 1.8$ and $\eta_{\max} > 1.8$, the shape of the neutron-tagged distribution is similar to that of the inclusive distribution; however, there are relatively fewer LRG events in the neutron-tagged sample. The LRG events represent only 4% of the total number of DIS events with neutrons in the measured kinematic region, but are 7% of the total number of DIS events. A reduction in the fraction of LRG events with a final-state neutron is expected since only proton diffractive dissociation or diffractive meson exchange (the Deck effect [65]) can contribute.

To investigate a possible x_L -dependence of the contribution of diffractive events, Fig. 17(b) shows the ratio, R_{LRG} , of the neutron-tagged DIS events, selected by the LRG criterion, to all neutron-tagged DIS events, as a function of x_L . The rise by a factor of three over the x_L range shows that the LRG neutron-tagged events have a harder neutron energy spectrum than that of the inclusive neutron-tagged sample. It is clear that diffractive events are not a major source of leading neutrons at any value of x_L . For the region $0.64 < x_L < 0.82$, R_{LRG} is 0.039 ± 0.001 (stat.);

- ρ and a_2 exchange

Theoretical studies of neutron production in ep collisions [18, 53] suggest that isovector exchanges other than the pion contribute less than 10% to neutron production at $x_L = 0.73$ and for the p_T range of the present data. This is quite different than for leading proton production, where isoscalar Regge exchange provides the dominant contribution [2, 19];

- isovector exchange leading to Δ production

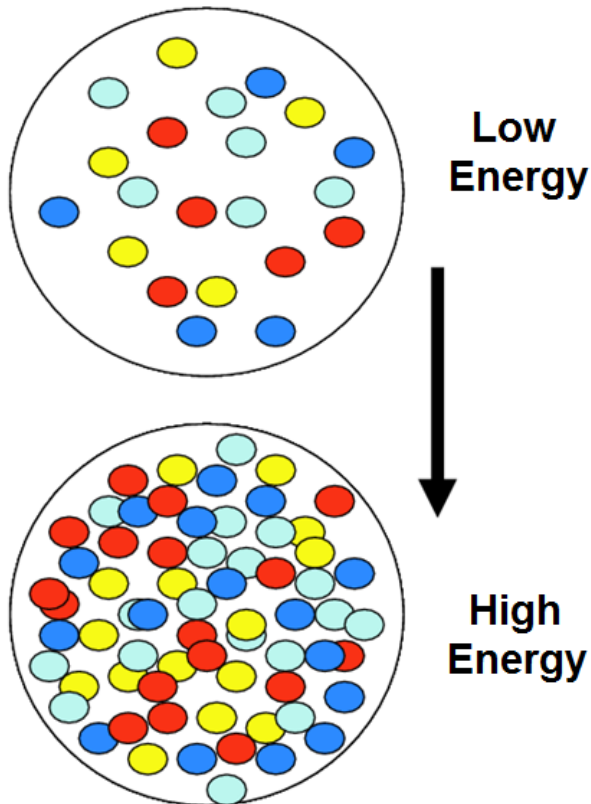
The $p \rightarrow \Delta(1236)$ transition, formed by π , ρ and a_2 exchange, can also contribute to neutron production [18, 53, 66–68]. In this case, the neutron, which comes from the decay $\Delta^0 \rightarrow n\pi^0$ or $\Delta^+ \rightarrow n\pi^+$, no longer has an energy determined by the energy of the exchanged meson. The neutron energy spectrum peaks near $x_L \approx 0.5$ and extends only to $x_L \approx 0.7$ [19]. It thus gives a small contribution in the $0.64 < x_L < 0.82$ bin. A comparison of the data on $p \rightarrow n$ and $p \rightarrow \Delta^{++}$ [69–72] in charge-exchange reactions at Fermilab indicates that only about 6% of the forward neutrons come from the Δ channel. This observation agrees with theoretical estimates of the $\Delta\pi$ contribution to the Fock state of the proton, which is approximately half that of $n\pi$ [53, 66]. A calculation [67] shows that the contribution of ρ/a_2 exchange, plus the Δ contribution, to the hadronic charge-exchange reaction $pp \rightarrow Xn$ could be as high as 30%. Since no analogous calculation exists for DIS, this only provides an indication of a possible background to the neutron production discussed in this paper;

- models other than one-particle exchange

Monte Carlo studies, using standard DIS generators, show [1] that these processes have a rate of neutron production a factor of three lower than the data and produce a neutron energy spectrum with the wrong shape, peaking at values of x_L below 0.3.

In summary, the expectation for the processes listed above at $\langle x_L \rangle = 0.73$ and $\langle p_T^2 \rangle = 0.08 \text{ GeV}^2$ is that they contribute of the order of 20% of the leading neutron production. This estimate can be checked using the measured neutron-energy spectrum. The OPE fit to the differential cross-section $d\sigma/dx_L$ shown in Fig. 8(a) suggests that, at $x_L = 0.73$, the residual background to OPE is $\lesssim 10\%$, in reasonable accord with the studies discussed above.

Gluon saturation

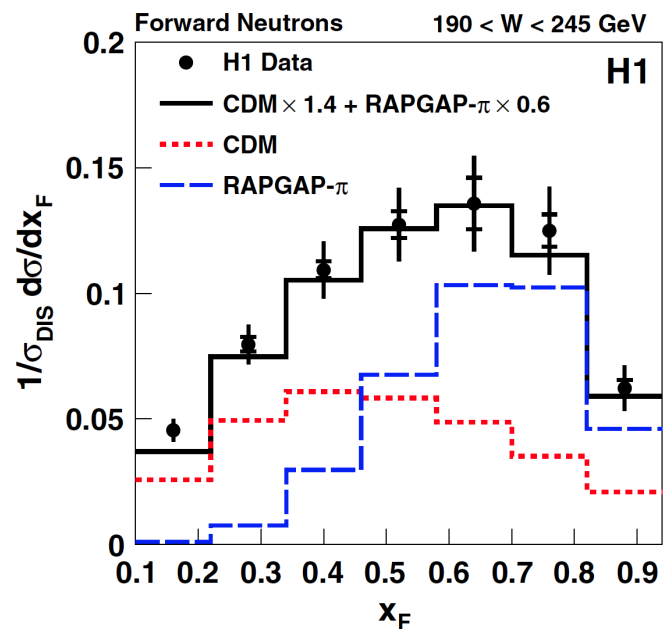
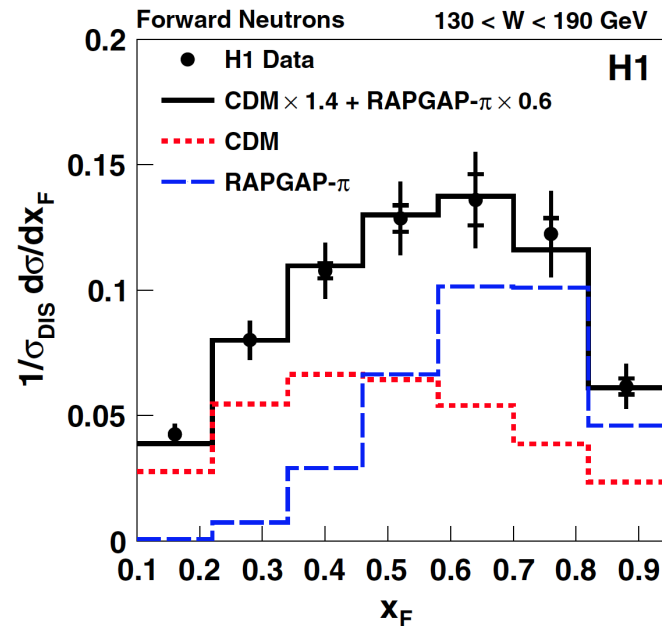
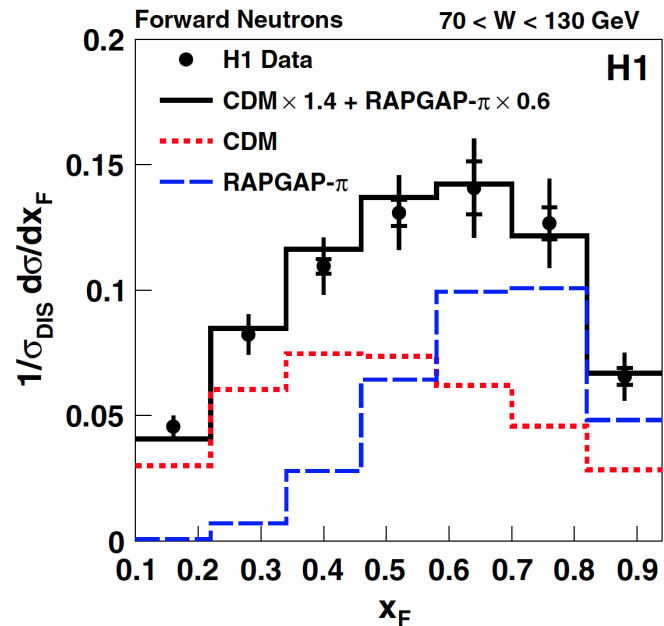


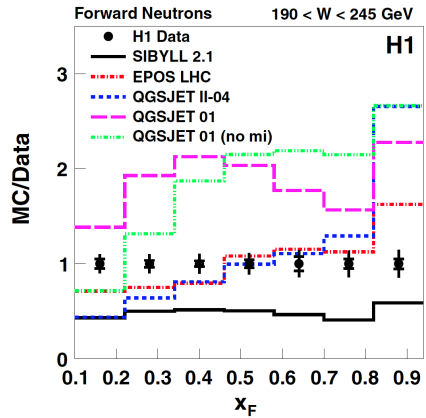
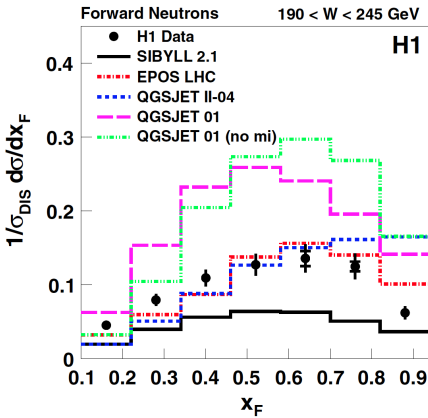
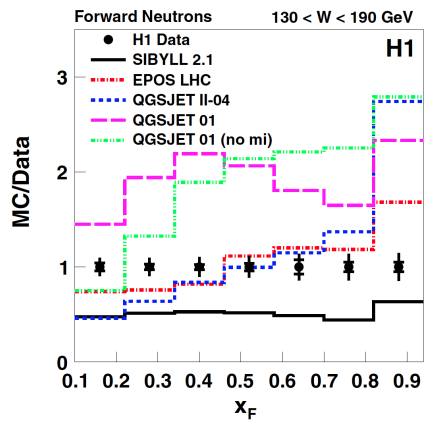
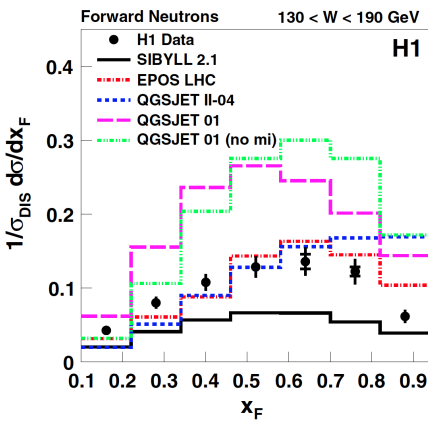
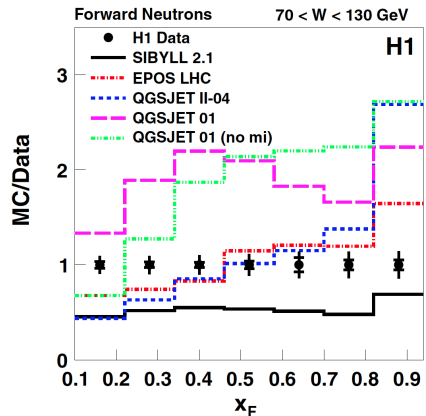
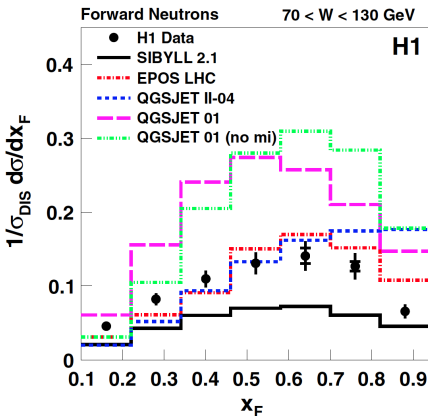
High energies
large number of gluons
gluon recombination

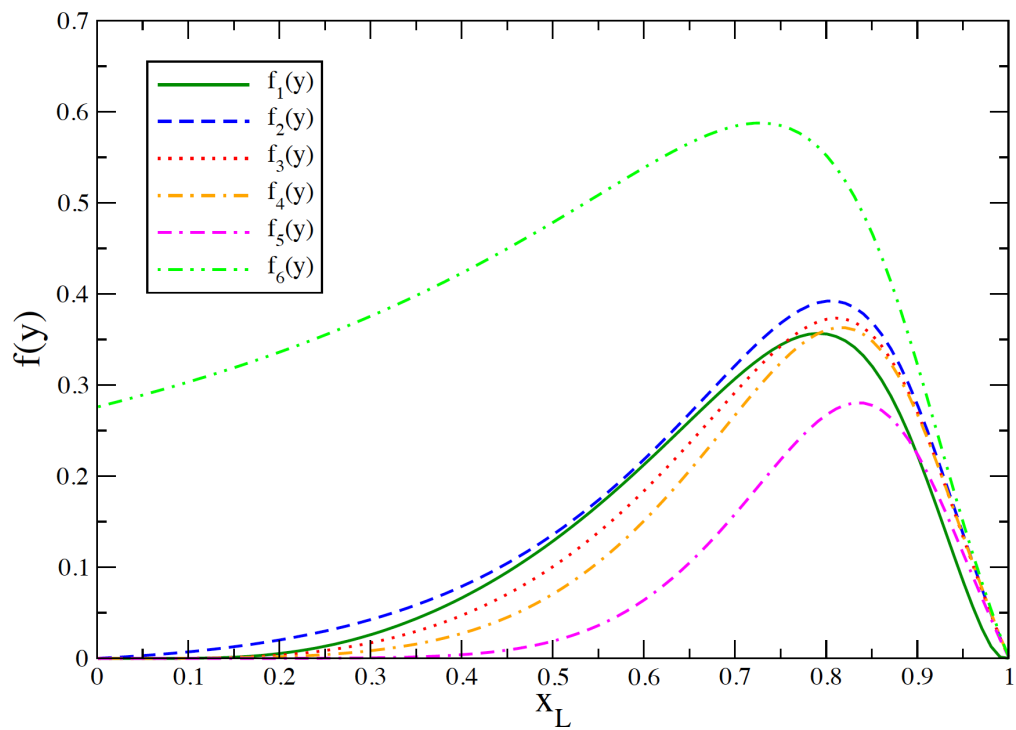
$$g g \rightarrow g$$

Gluon recombination at very small x tames the growth of the gluon distribution

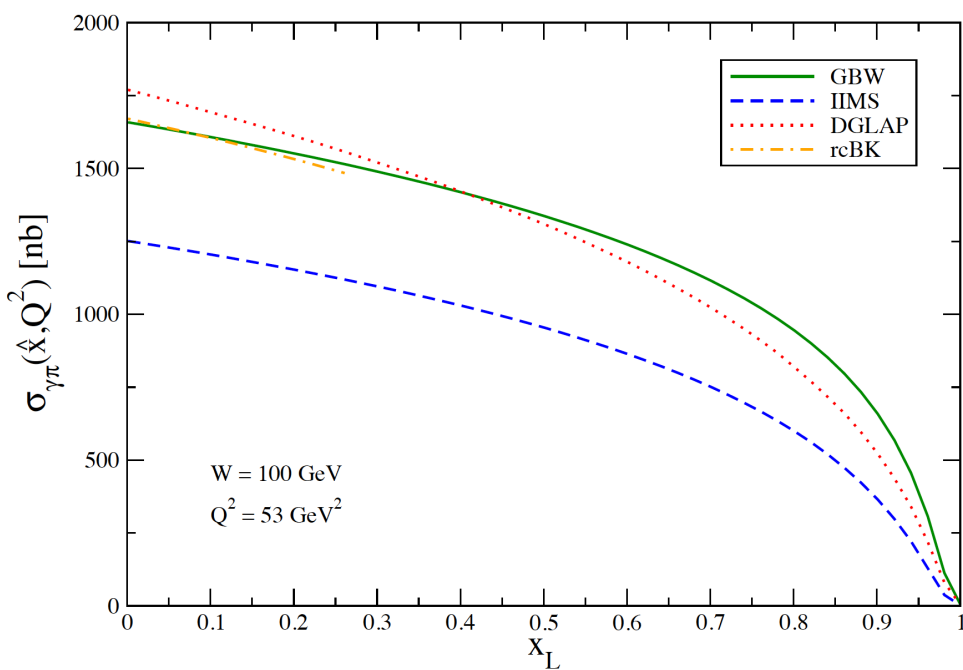
Implementation: color dipole approach



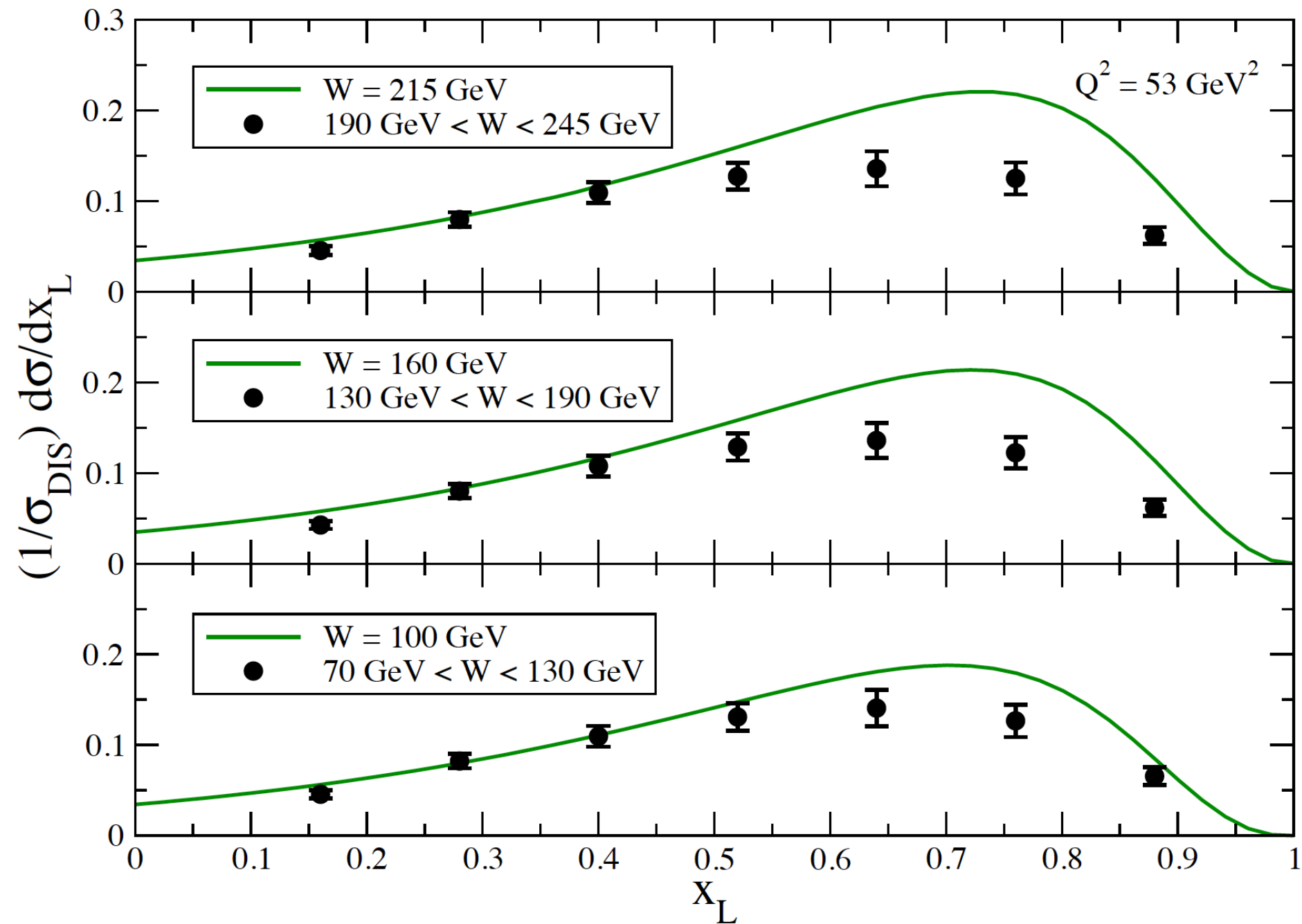




Flux factor



Dipole cross section



$$\hat{x} = \frac{Q^2 + m_f^2}{\hat{W}^2 + Q^2} = \frac{Q^2 + m_f^2}{(1 - x_L)W^2 + Q^2}$$

Leading neutron production
can be low x physics !

